European Journal of Medicinal Chemistry 212 (2021) 113045

Contents lists available at ScienceDirect

European Journal of Medicinal Chemistry

journal homepage: http://www.elsevier.com/locate/ejmech

Research paper

Rational drug design of 6-substituted 4-anilino-2-phenylpyrimidines for exploration of novel ABCG2 binding site

Katja Silbermann [2], Jiyang Li [2], Vigneshwaran Namasivayam [2], Sven Marcel Stefan[**,1], Michael Wiese[*]

Pharmaceutical and Cellbiological Chemistry, Pharmaceutical Institute, Rheinische Friedrich-Wilhelms-University of Bonn, An der Immenburg 4, 53121, Bonn, Germany

ARTICLE INFO

Article history:
Received 1 September 2020
Received in revised form
18 November 2020
Accepted 21 November 2020
Available online 3 December 2020

Keywords:
ABCG2 (BCRP)
ABCB1 (*P*-gp)
ABCC1 (MRP1)
Multidrug resistance (MDR)
Dual inhibition
Promiscuous inhibitor
Multitarget antagonist
Broad-spectrum antagonism

ABSTRACT

In the search for novel, highly potent, and nontoxic adjuvant chemotherapeutics to resolve the major issue of ABC transporter-mediated multidrug resistance (MDR), pyrimidines were discovered as a promising compound class of modern ABCG2 inhibitors. As ABCG2-mediated MDR is a major obstacle in leukemia, pancreatic carcinoma, and breast cancer chemotherapy, adjuvant chemotherapeutics are highly desired for future clinical oncology. Very recently, docking studies of one of the most potent reversers of ABCG2-mediated MDR were reported and revealed a putative second binding pocket of ABCG2. Based on this (sub)pocket, a series of 16 differently 6-substituted 4-anilino-2-phenylpyrimidines was designed and synthesized to explore the potential increase in inhibitory activity of these ABCG2 inhibitors. The compounds were assessed for their influence on the ABCG2-mediated pheophorbide A transport, as well as the ABCB1- and ABCC1-mediated transport of calcein AM. They were additionally evaluated in MDR reversal assays to determine their half-maximal reversal concentration (EC_{50}). The 6-substitution did not only show increased toxicity against ABCG2-overexpressing cells in combination with SN-38 but also a negative influence on cell viability in general. Nevertheless, several candidates had EC_{50} values in the low double-digit nanomolar concentration range, qualifying them as some of the most potent reversers of ABCG2-mediated MDR. In addition, five novel multitarget ABCB1, ABCC1, and ABCG2 inhibitors were discovered, four of them exerting their inhibitory power against the three stated transporters at least in the single-digit micromolar concentration range.

1. Introduction

The ABC transport protein breast cancer resistance protein (ABCG2, BCRP) is recognized as a negative marker in (relapsed/refractory) cancer in general. It is associated with decreased progression- or disease-free survival and increased mortality [1–4], as well as the development of metastases [5]. Its expression was determined in several cancers, such as leukemia [3,4,6], pancreatic carcinoma [2,6], or breast cancer [6]. Like ABCB1 (*P*-glycoprotein, *P*-gp) and ABCC1 (multidrug resistance-associated protein 1, MRP1), ABCG2 recognizes applied antineoplastic agents inside the cancer cell as well as in the cell membrane and extrudes these into the exterior at the expense of the energy source ATP [7]. This results in the resistance of the respective cancer cells to chemotherapeutic drugs. Moreover, resistance to other first- and second-line antineoplastic agents is observed that were not used *a priori* in anticancer regimens. This so-called cross-resistance is concomitant

Abbreviations: A2780/ADR, adriamycin-(doxorubicin)-selected A2780 cells; ABC, ATP-binding cassette; ATP, adenosine-triphosphate; BCRP, breast cancer resistance protein; calcein AM, calcein acetoxymethyl ester; CsA, cyclosporine A; cryo-EM, cryogenic electron microscopy; EC_{50}, half-maximal reversal concentration; GFP, green fluorescent protein; GI_{50}, half-maximal growth inhibition concentration; I_{max}, maximal inhibition level; MDCK, madin-darby canine kidney; MTT, 3-(4,5-dimethylthiazol-2-yl)-2,5-diphenyltetrazolium bromide; MDR, multidrug resistance; MRP1, multidrug resistance-associated protein 1; *P*-gp, *P*-glycoprotein; °s, degree of sensitization; SEM, standard error of the mean; sr, selectivity ratio; TKI, tyrosine kinase inhibitor; tr, therapeutic ratio; v_{max}, maximal transport velocity.

* Corresponding author.
** Corresponding author.
E-mail addresses: s.m.stefan@medisin.uio.no (S.M. Stefan), mwiese@uni-bonn.de (M. Wiese).
[1] Present author address: Sven Marcel Stefan, Translational Neurodegeneration Research and Neuropathology Lab, Department of Neuro-/Pathology, University of Oslo, Oslo, Norway.
[2] These three authors contributed equally to this work.

https://doi.org/10.1016/j.ejmech.2020.113045
0223-5234/

with the overexpression of ABC transport proteins, and the associated phenomenon was designated as 'multidrug resistance' (MDR). With respect to ABCG2, cross-resistance against several antineoplastic agents of structural diversity has been described, such as camptothecins, epipodophyllotoxins, mitoxantrone, or tyrosine kinase inhibitors (TKIs) [6–8].

The latter compound class comprises of compounds with common structural features, such as quinazoline (e.g., canertinib [9], **1**), quinoline (e.g., pelitinib [10], **2**), pyrimidine (e.g., ceritinib [11], **3**), or pyridine (e.g., apatinib [12], **4**). TKIs have a special standing with regard to ABCG2 inhibition, which becomes clear when focusing on the stated examples, which are depicted in Fig. 1: In 2001, canertinib was the very first TKI proven to interact with ABCG2 in an inhibitory way, which made it one of the first ABCG2 inhibitors [9]; pelitinib is one of only around 75 multitarget reversers of ABCB1-, ABCC1-, and ABCG2-mediated MDR known until today [10,13–24]; ceritinib is the most potent TKI-related (selective) reverser of ABCG2-mediated MDR [11]; and apatinib is a very rare example of an TKI that made it into the clinic in combination with another antineoplastic agent [25].

Starting from the above stated compounds, our workgroup was able to develop several new potent inhibitors of ABC transporters in general, and of ABCG2 in particular. Until today, compound **5** with its quinazoline scaffold is one of the most potent inhibitors of ABCG2 [26]; Compound **6** with its quinoline scaffold is one of the 20 most potent multitarget ABCB1, ABCC1, and ABCG2 inhibitors [11,15,27–36]; the consequent downsizing of the main scaffold to a pyrimidine led to the discovery of compound **7** as a novel ABCG2 inhibitor [37]; and subsequent development of small-molecule pyrimidines led to one of the most potent reversers of ABCG2-mediated MDR, compound **8** [17]. Fig. 2 shows the stated compounds **5**–**8**.

In case of both compound classes quinazolines and pyrimidines, the inhibition type could be determined as competitive with respect to the ABCG2-mediated transport of Hoechst 33342 [17,26,37], and our studies with structure-based drug design approaches proposed the binding behavior of both scaffolds [17,26]. Interestingly, a binding (sub)pocket has opened up in the case of compound **8** [17], which forms the basis for the current study. In order to evaluate the (sub)pocket we designed and synthesized compounds to enhance their potency and selectivity against ABCG2 as well as their capability to reverse ABCG2-mediated resistance against SN-38.

2. Results and discussion

2.1. ABCG2–compound 8 complex analysis

Recently, on the basis of the cryo-electron microscopy (cryo-EM) structure of human ABCG2 and docking studies [38,39], the putative binding mode of Hoechst 33342 was reported [26]. The studies were extended to explore the binding mode of the potent quinazoline inhibitors of ABCG2 and to explain the mechanism of inhibition [17,26]. Very recently, pyrimidine based ABCG2 inhibitors showed excellent inhibitory potency and antiproliferative efficacy [17]. The docking studies explained the binding mode and their interaction with the amino acid residues in the pocket, which was in agreement with the competitive mode of inhibition against the substrate Hoechst 33342 (Fig. 3A and B). The pyrimidine scaffold formed interactions with Asn387 and Asn391, the amino linker formed an interaction with Glu451, the substituted phenyl ring was positioned in the hydrophobic (sub)pocket, and the cyano substituent formed strong electrostatic interaction with Arg191 (Fig. 3C). The binding pose of the potent pyrimidine scaffold **8** suggested a

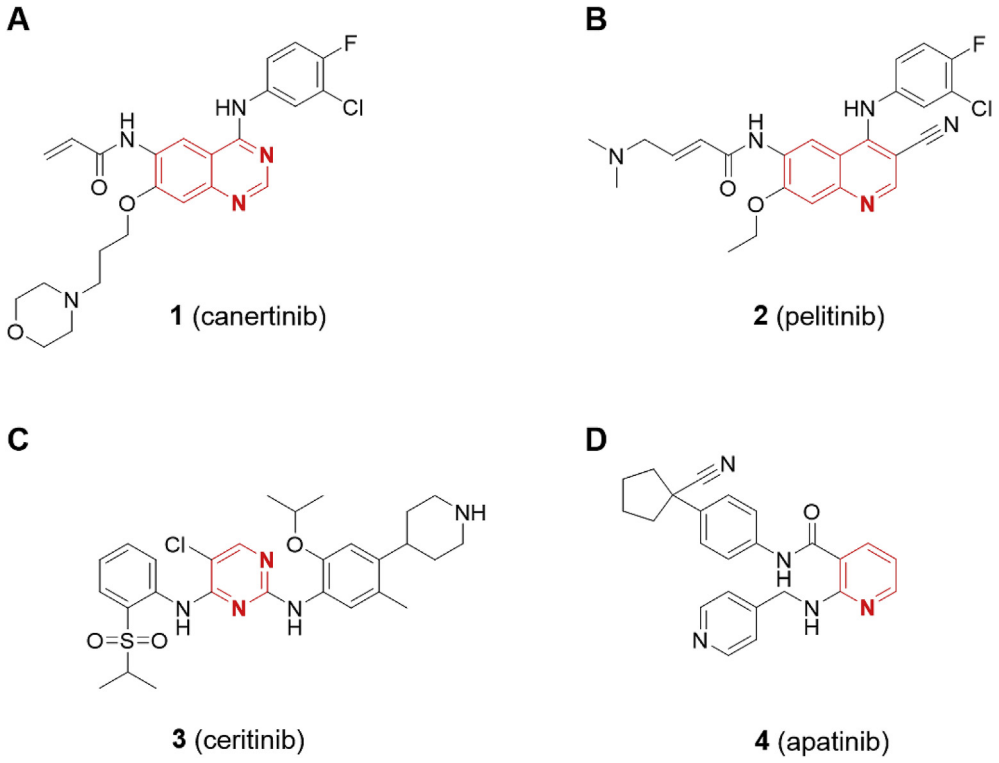

Fig. 1. 2D representation of famous TKIs reported in the context of ABCG2 inhibition. (A) The very first TKI associated with ABCG2 inhibition, canertinib (**1**) [9]; (B) one of only around 75 known (multitarget) reversers of ABCB1-, ABCC1-, and ABCG2-mediated MDR, pelitinib (**2**) [10]; (C) the most potent TKI-related selective reverser of ABCG2-mediated MDR, ceritinib (**3**) [11]; one of the rare TKIs used in combination with another antineoplastic agent (and ABCG2 substrate), apatinib, in an anticancer regimen (**4**) [25].

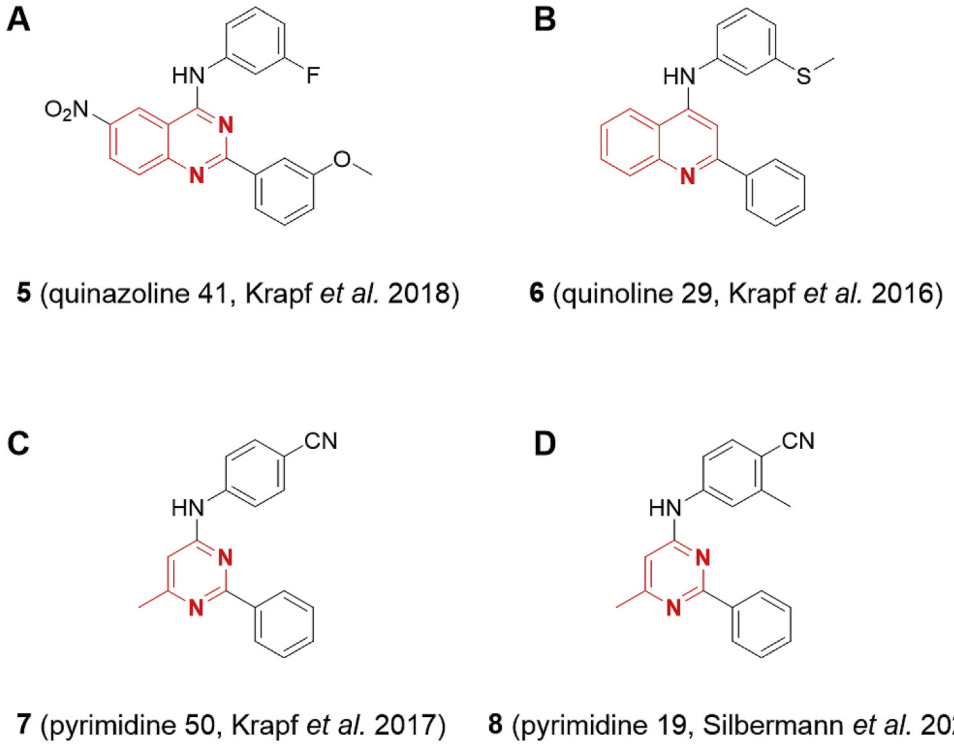

Fig. 2. Depiction of recent advances in the development of ABCG2 inhibitors. (A) One of the most potent ABCG2 inhibitors, quinazoline 41 (**5**; $IC_{50\ (ABCG2)} = 23.4$ nM) [26]; (B) one of the 20 most potent multitarget ABCB1, ABCC1, and ABCG2 inhibitors, quinoline 29 (**6**; $IC_{50\ (ABCB1)} = 1.42$ μM; $IC_{50\ (ABCC1)} = 2.98$ μM; $IC_{50\ (ABCG2)} = 1.90$ μM) [27]. (C) one of the first reported ABCG2 inhibitors with pyrimidine core structure, pyrimidine 50 (**7**; $IC_{50\ (ABCG2)} = 71.4$ nM) [37]; and one of the most potent reversers of ABCG2-mediated MDR as reported recently, pyrimidine 19 (**8**; $EC_{50\ (ABCG2)} = 11.0$ nM) [17].

(sub)pocket lined by Gln18, Phe182, and Glu446 closer to the methyl substitution at position 6 (Fig. 3C). In this work, the (sub) pocket was explored with different substitutions including alkyl, aromatic, and substituted aromatic side chains at position 6 of the pyrimidine core structure.

2.2. Chemistry

The 6-substituted 4-anilino-2-phenylpyrimidine derivatives were synthesized in four steps. First, benzamidine was condensed with diethyl malonate in a freshly prepared sodium ethoxide solution to form the pyrimidine scaffold (**9**). Second, intermediate **9** was refluxed in phosphorous oxychloride to yield the chlorinated precursor **10**. Third, compound **10** was treated with one equivalent of 4-cyanoaniline to yield the monosubstituted product **11** under catalyzation with 0.1 equivalent of concentrated hydrochloric acid. Finally, the desired compounds were synthesized by exposing precursor **11** with differently substituted amines (**12**–**15**), anilines (**17**–**27**) or phenylboric acid (via Suzuki coupling in the presence of a palladium catalyst and base; **16**). Scheme 1 summarizes the prevailing reaction steps.

2.3. Biological investigation

2.3.1. Determination of inhibitory activity against ABCG2

The inhibitory activity of the synthesized compounds **12**–**27** against ABCG2 was investigated in a pheophorbide A assay using ABCG2-overexpressing MDCK II BCRP cells as already described earlier [15–17,40,41].

In this assay, blockage of ABCG2-mediated pheophorbide A transport leads to the enhanced intracellular presence of this fluorescence dye proportionate to the degree of inhibition. The standard ABCG2 inhibitor Ko143 [(3*S*,6*S*,12a*S*)-1,2,3,4,6,7,12,12a-octahydro-9-methoxy-6-(2-methylpropyl)-1,4-dioxopyrazino[1′,2′:1,6]pyrido[3,4-*b*]indole-3-propanoic acid 1,1-dimethylethyl ester; **28**] was used as reference to determine the maximum inhibition level (I_{max}). Table 1 summarizes the obtained half-maximal inhibition concentrations (IC_{50}) and I_{max} values. In addition, the corresponding IC_{50} values of compounds **7** and **8** are shown for comparison as taken from the literature [17,37].

On the basis of the docking studies [17,26] we synthesized compound set (i) with different alkyl residues linked to the pyrimidine moiety by an amino linker (**12**–**15**). Here, the methylamino derivative **12** ($IC_{50} = 0.141$ μM) exceeded the inhibitory activity of the parent compound **7** ($IC_{50} = 0.189$ μM) as well as the reference compounds **8** ($IC_{50} = 0.175$ μM) and **28** ($IC_{50} = 0.274$ μM), but with a slight decrease of I_{max}. Larger residues such as isopropylamino (**13**) or butylamino (**15**) were less preferred, while on the other hand a *n*-propyl substituent (**14**) resulted in notable inhibitory activity ($IC_{50} = 0.293$ μM), which was slightly inferior to that of compound **7**, while I_{max} equaled that of reference **28** (Fig. 4A).

Possibly the aliphatic side chains open up only limited potential for lipophilic interactions with the target and can adopt different orientations in the binding pocket due to their high flexibility. This questions whether aromatic and/or aromatic-aliphatic side chains would be beneficial for inhibitory activity against ABCG2. Therefore, compound set (ii) was synthesized (**16**–**20**). Interestingly, a phenyl ring without amino linker (**16**) resulted in great loss of inhibitory activity. Its amino analog **17** ($IC_{50} = 0.169$ μM) was nearly as potent as the corresponding methylamino derivative **12**, and slightly superior to the parent compound **7**. While the insertion of a methylene linker (**18**) resulted in a weaker inhibitory activity, a propylene linker boosted the inhibitory potency, making the

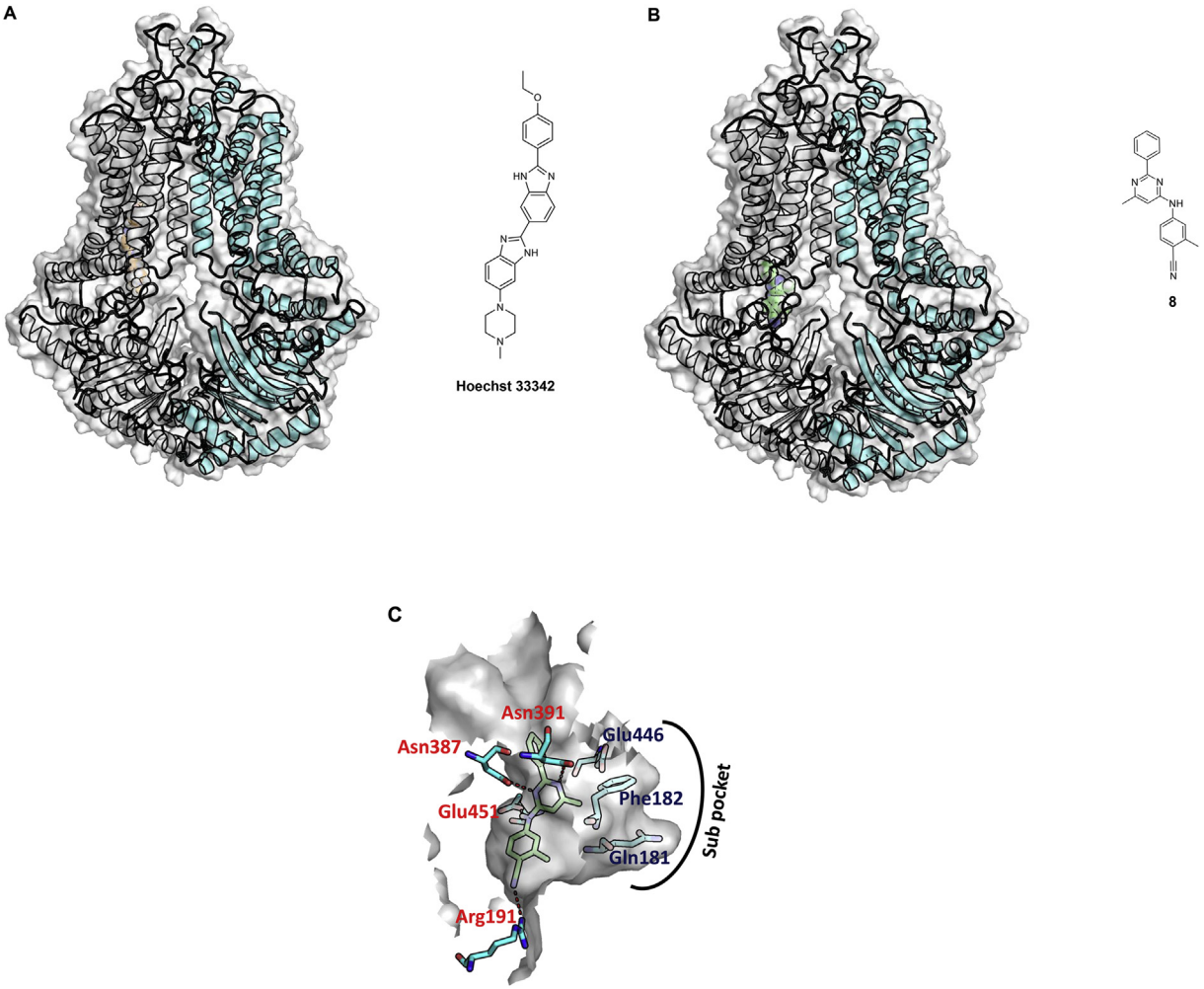

Fig. 3. Putative binding modes of Hoechst 33342 and compound **8**. The docked pose of (A) the ABCG2 substrate Hoechst 33342 (carbon colored orange, represented as spheres) and (B) the ABCG2 inhibitor compound **8** (carbon colored green, represented as spheres) in the binding pocket of human ABCG2 represented in cartoon and colored chain A and B in grey and cyan, respectively. The chemical structures of (A) Hoechst 33342 and (B) compound **8** are provided. (C) The binding pocket of compound **8** with the important amino acid residues (label colored red) interacting with compound **8** (colored in green) and the residues in the additional (sub)pocket (label colored blue) represented as sticks and colored in cyan are shown. The interactions of compound **8** with amino acid residues in the binding pocket are colored in red dashed lines. Oxygen atoms are colored in red, nitrogen atoms in blue, and polar hydrogen atoms of compound **8** are colored in white.

corresponding compound **19** the most potent within this manuscript (IC_{50} = 0.0960 μM; Fig. 4B). This shows that there is a need for an optimal linker to position the larger aromatic substituent into the binding pocket.

Interestingly, compound **20** with its phenylbutylamino substituent was only marginally weaker than compound **19**, which appears to contradict the finding that a butyl chain is much less favorable than a propyl chain (**14** vs **15**). This could be explained by two things: first, compound **19** found good interaction with the residues in the binding pocket (possibly Phe182) according to the chain length and the resulting orientation of the phenyl ring; second, the butyl chain indeed hampers interaction, but subsequently leads to an even better orientation of the phenyl ring, thus, leading to a compensation of these two effects. However, it should be noted that the I_{max} value of both compounds **19** and **20** was rather low (61% each).

In the next step, the effect of a nitrogen-containing aromatic ring system was investigated. Therefore, compound set (iii) comprising of pyrimidines **21**–**23** was synthesized. The 2-pyridylamino derivative **21** had a notable inhibitory activity (IC_{50} = 0.210 μM) against ABCG2 comparable to its phenyl counterpart **17** as well as reference compounds **7** and **8**, while the 3- (**22**) and 4-pyridylamino (**23**) derivatives showed less pronounced inhibition. This suggests that the positioning of the nitrogen atom is important and it could form an interaction with Gln181 when it was placed at position 2 of the aromatic ring.

Since hydroxy- and cyano-anilino pyrimidine derivatives showed a marked inhibitory activity against ABCG2 in our previous studies [17,37], these substituents were inserted at position 6 to further evaluate the new (sub)pocket [compound set (iv); **24**–**27**]. Comparable to the correlation given for the pyridine derivatives **21**–**23**, the 2-hydroxyaniline derivative **24** was the most potent representative of this sub-set (IC_{50} = 0.223 μM) followed by its 4-hydroxyaniline derivatives **26** (IC_{50} = 0.387 μM) and 3-hydroxyaniline analog **25** (IC_{50} = 0.608 μM). Interestingly, the 4-cyano derivative **27** was found to be one of the most potent compounds within the investigated compounds (IC_{50} = 0.133). It exceeded not only the inhibitory activities of the parent and reference compounds **7**, **8**, and **28**, but also the lead molecules of the corresponding compound classes, **12** (i), **17** (ii), and **21** (iii). It was only slightly less potent than compound **19**, but had an inferior I_{max} compared to the latter. This is possible as the hydroxy substitution

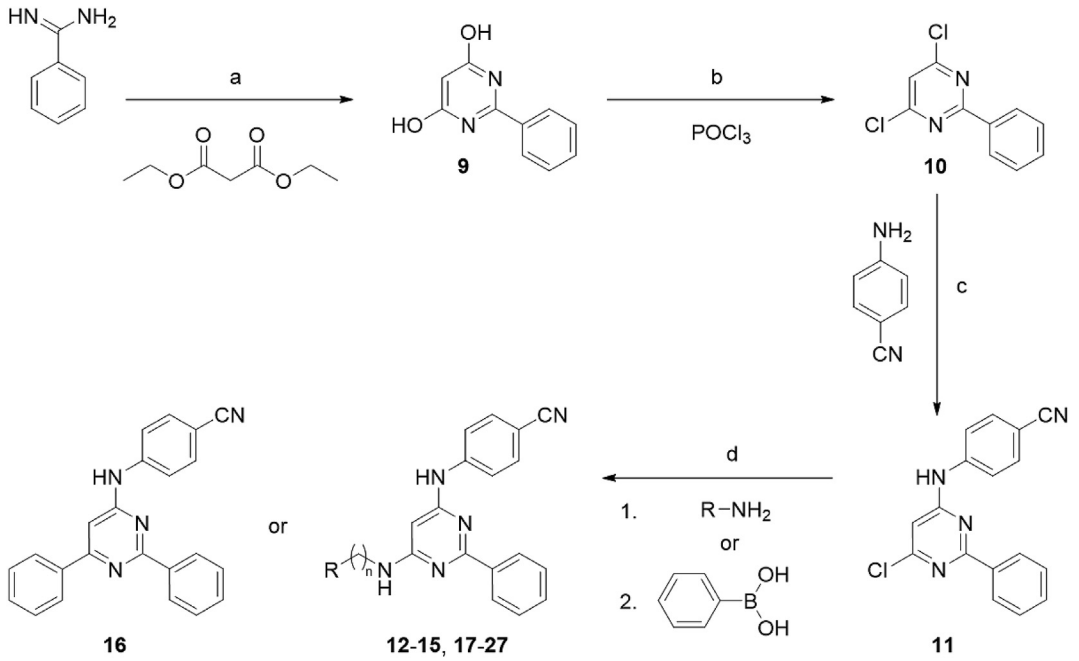

Scheme 1. General synthesis of 6-substituted 4-anilino-2-phenylpyrimidine derivatives. Reagents and conditions: (a) NaOEt/EtOH, reflux, overnight; (b) $POCl_3$, reflux, 8–9 h; (c) *i*-PrOH, HCl-catalyzed, reflux, overnight; (d) 1. *i*-PrOH, microwave-assisted, 110 °C, 0.5 h; 2. dioxane, 2 M K_2CO_3 (3:1), Pd(*t*-$Bu_3P)_2$-catalyzed, argon, 90 °C, 7 h.

of compounds **24** and **26** at positions 2 and 4, respectively, and the 4-cyano (**27**) might introduce hydrogen bond interactions with Glu446 or Gln181, while the hydroxyl substitution at position 3 (**25**) might alter the orientation of the compound in the binding pocket.

2.3.2. Determination of selectivity against ABCB1 and ABCC1

The synthesized compounds were evaluated for their inhibitory activity against two other major important targets in ABC transporter-mediated MDR, namely ABCB1 and ABCC1. For this purpose, a calcein AM assay was conducted using either ABCB1-overexpressing A2780/ADR or ABCC1-overexpressing H69AR cells as described earlier [15–17,40,41]. In short, the highly lipophilic calcein AM enters the cell by passive diffusion and gets effluxed by either ABCB1 or ABCC1. In case of ABCB1 or ABCC1 inhibition, the calcein AM persists inside the cell and gets cleaved by unspecific intracellular esterases to the fluorescence dye calcein. As mentioned above for the pheophorbide A assay, the degree of inhibition of either ABCB1 or ABCC1 is proportionately correlated to the amount of measured fluorescence of calcein. The compounds have been evaluated at a concentration of 10 μM, and for representatives with effect values ≥ 20% (+SEM) compared to the standard ABCB1 and ABCC1 inhibitor, cyclosporine A (CsA; 10 μM), complete concentration-effect curves have been generated and their IC_{50} values were calculated. The results of the corresponding screening can be seen in Fig. 5A (ABCB1) and 5B (ABCC1), while the associated values are presented in Table 2.

Compared to the results in Table 1, the methylamino derivative **12** showed only minor inhibitory activity against ABCB1 ($IC_{50\ (ABCB1)}$ = 25.9 μM) and none against ABCC1, suggesting that this compound is a selective and highly potent ABCG2 inhibitor. The inhibitory activities of compounds **13** and **14** revealed both as moderately potent multitarget ABCB1, ABCC1, and ABCG2 inhibitors. The butylamino derivative **15** was discovered as a dual ABCB1 and ABCG2 inhibitor ($IC_{50\ (ABCB1)}$ = 6.62 μM), although it must be stated that its affinity to ABCG2 was over 13 times higher than to ABCB1.

While compound set (ii) contained no compound with noteworthy inhibitory power against ABCC1, compounds **17** and **18** were shown to be dual ABCB1 and ABCG2 inhibitors, but as already stated for compound **15**, both the benzyl and phenethyl derivatives **17** ($IC_{50\ (ABCB1)}$ = 5.38 μM) and **18** ($IC_{50\ (ABCB1)}$ = 4.47 μM) were 32 and 16 times weaker with regard to ABCB1 inhibition.

The 6-pyridyl pyrimidines **21**–**23** were found to be dual ABCB1 and ABCG2 inhibitors with a 16 (**21**; $IC_{50\ (ABCB1)}$ = 3.40 μM), 15 (**22**; $IC_{50\ (ABCB1)}$ = 5.41 μM), and 10 (**23**; $IC_{50\ (ABCB1)}$ = 4.26 μM) times higher inhibitory activity against ABCG2, respectively. Indeed, compound **22** had slight inhibitory power against ABCC1 ($IC_{50\ (ABCC1)}$ = 20.7 μM), which made it a rare example of a triple ABCB1, ABCC1, and ABCG2 inhibitor, but considering its 56 times lower affinity toward ABCC1, it is *de facto* a dual ABCB1 and ABCG2 inhibitor.

Compound set (iv) was quite diverse according to its interaction profile: While the 2-hydroxyphenylamino derivative **24** was shown to be a dual ABCB1 and ABCG2 inhibitor with 13 times higher affinity to the latter transporter ($IC_{50\ (ABCB1)}$ = 2.98 μM); compounds **25** ($IC_{50\ (ABCB1)}$ = 3.52 μM; $IC_{50\ (ABCC1)}$ = 4.08 μM) and **26** ($IC_{50\ (ABCB1)}$ = 4.54 μM; $IC_{50\ (ABCC1)}$ = 4.04 μM) are special representatives of broad-spectrum ABCB1, ABCC1, and ABCG2 inhibitors in low single-digit and submicromolar concentration range, belonging to the 22 most potent of its kind [11,15,27–36]; and the second most potent ABCG2 inhibitor **27** can be considered ABCG2-selective as its affinity to ABCB1 is over 50 times less (IC_{50} = 6.75 μM).

In summary, the presented results highlight the most potent ABCG2 inhibitors **12**, **17**, **19**–**20** and **27** as selective, while compounds **13**–**14** and **25**–**26** represent limited examples of broad-spectrum ABCB1, ABCC1, and ABCG2 inhibitors. Compound **24** is a good representative of a dual ABCB1 and ABCG2 inhibitor.

2.3.3. Determination of intrinsic toxicity in MDCK II BCRP and MDCK II cells

The intrinsic cytotoxicity of the cells was evaluated by performing a MTT-(3-(4,5-demethyl-2-thiazolyl)-2,5-diphenyl-2H-

Table 1
Inhibitory activity of 6-substituted 4-anilino-2-phenylpyrimidine derivatives obtained in a pheophorbide A assay using ABCG2-overexpressing MDCK II BCRP cells as described earlier [15–17,40,41]. IC_{50} and I_{max} values are expressed as mean ± standard error of the mean (SEM) of at least three independent experiments.

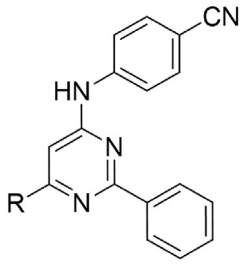

No	R	IC_{50} ± SEM [μM] MDCK II BCRP	I_{max} ± SEM [%] MDCK II BCRP
7		0.189 ± 0.022[a]	87 ± 8[a]
8		0.175 ± 0.011[b]	76 ± 12[b]
12	methylamino	0.141 ± 0.029	68 ± 8
13	*i*-propylamino	0.763 ± 0.088	101 ± 6
14	*n*-propylamino	0.293 ± 0.043	89 ± 8
15	*n*-butylamino	0.500 ± 0.034	73 ± 9
16	phenyl	4.41 ± 0.13	100[c]
17	anilino	0.169 ± 0.010	84 ± 14
18	benzylamino	0.283 ± 0.025	99 ± 11
19	phenylpropylamino	0.0960 ± 0.0162	61 ± 7
20	phenylbutylamino	0.147 ± 0.021	61 ± 1
21	2-pyridylmethylamino	0.210 ± 0.004	88 ± 4
22	3-pyridylmethylamino	0.373 ± 0.023	91 ± 4
23	4-pyridylmethylamino	0.435 ± 0.001	78 ± 11
24	2-hydroxyanilino	0.223 ± 0.013	86 ± 10
25	3-hydroxyanilino	0.608 ± 0.028	66 ± 9
26	4-hydroxyanilino	0.387 ± 0.036	76 ± 4
27	4-cyanoanilino	0.133 ± 0.014	60 ± 3
28		0.274 ± 0.014	100

[a] Compound **7** has been reported before in a Hoechst 33342 assay (IC_{50} = 71.4 nM) [37]; the inhibitory potency has been determined in the pheophorbide A assay.
[b] Data for compound **8** as reported in the literature [17].
[c] Constrained to I_{max} of compound **28**.

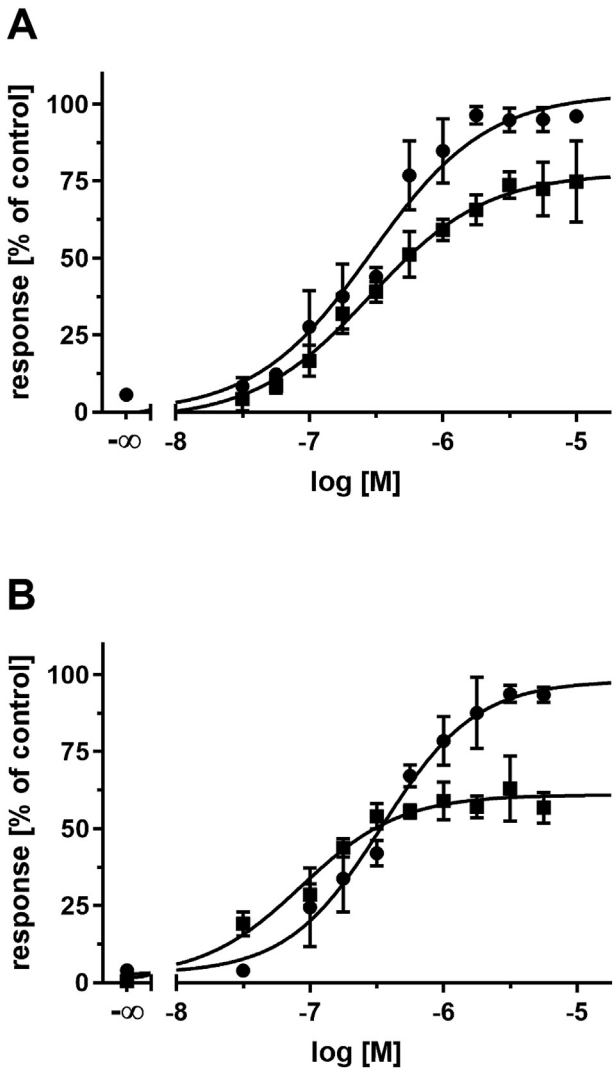

Fig. 4. Concentration-effect curves of compounds **14** (A; closed squares; IC_{50} = 0.293 μM) and **19** (B; closed squares; IC_{50} = 0.0960 μM) in comparison to reference inhibitor **28** (A,B; closed circles; IC_{50} = 0.274 μM) applying a pheophorbide A accumulation assay. The data are shown as mean ± SEM of at least three independent experiments.

tetrazolium bromide)-based cell viability assay applying the same cells that were used for the inhibition assays, MDCK II BCRP and MDCK II, as already described [15–17,41]. Pure culture medium served as a reference for 100% cell viability and 10% DMSO was chosen as a positive control (0% cell viability). To determine the half-maximal growth inhibition (GI_{50}) values, complete concentration-effect curves have been generated. Table 3 summarizes the obtained results including the therapeutic ratio (tr) using the inhibition values as reported in Table 1.

In general, the compound class of 6-substituted 4-anilino-2-phenylpyrimidines seems to impair cell viability as can be visualized from the rather low GI_{50} values in the mid-single-digit concentration range. Considering the very selective and highly potent representatives **12**, **17**, **19**–**21**, **24**, and **27**, only compounds **12**, **20**, and **27** had acceptable therapeutic ratios of over 50 (180, 65.0, and 58.7, respectively), which gives these three compounds a special standing among the presented compounds. Unfortunately, the most potent ABCG2 inhibitor **19** turned out to be one of the most toxic compounds within the four sets, not only regarding its tr (38.4), but especially due to its absolute GI_{50} values of 3.64 μM (MDCK II BCRP) and 5.03 μM (MDCK II), which are amongst the lowest measured values of all. Both extremes, the rather nontoxic compound **12** and the most potent but most toxic compounds **19** are shown in Fig. 6.

2.3.4. Determination of intrinsic toxicity using A2780/ADR, A2780, and H69AR cells

As compound **24** was found to be a moderately good dual ABCB1 and ABCG2 inhibitor, and compounds **13**–**14** as well as **25**–**26** were discovered as multitarget ABCB1, ABCC1, and ABCG2 inhibitors, their intrinsic toxicity has also been assessed using A2780/ADR, A2780, and H69AR cells applying the MTT-based cell viability assay as described above [15–17,40,41]. The obtained GI_{50} values are presented in Table 4.

The GI_{50} values of the dual ABCB1 and ABCG2 inhibitor **24** and triple ABCB1, ABCC1, and ABCG2 inhibitors **13**–**14** and **25**–**26** are rather low and can be compared to the values determined for the MDCK II BCRP and MDCK II cells (Table 3). Since the inhibition values of compound **24** against ABCB1 and compounds **13**–**14** as well as **25**–**26** against ABCB1 and ABCC2 were in the mid-single-digit micromolar concentration range, it could be expected that their tr is suboptimal.

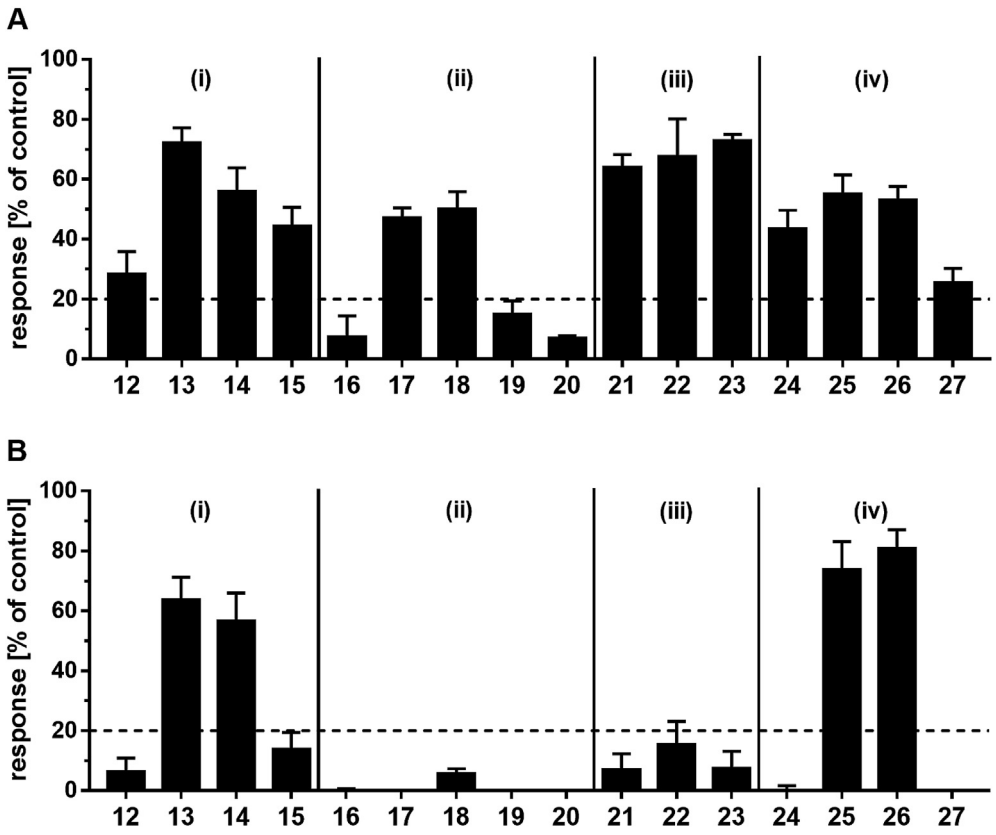

Fig. 5. Screening of 6-substituted 4-anilino-2-phenylpyrimidine sets (i)-(iv) at 10 μM against ABCB1, using the ABCB1-overexpressing cell line A2780/ADR (A), and ABCC1, applying the ABCC1-overexpressing cell line H69AR (B), conducted with a calcein AM assay as described earlier [15–17,40,41]. CsA (10 μM) has been used as a reference which defined 100% inhibition, while buffer medium served as a negative control (0%). Shown is mean ± SEM of at least three independent experiments.

Table 2
Inhibitory activity of 6-substituted 4-anilino-2-phenylpyrimidine derivatives obtained in a calcein AM assay using either ABCB1-overexpressing A2780/ADR or ABCC1-overexpressing H69AR cells as described earlier [15–17,40,41]. IC_{50} values are expressed as mean ± SEM of at least three independent experiments.

No	R	IC_{50} ± SEM [μM] A2780/ADR	IC_{50} ± SEM [μM] H69AR
12	methylamino	25.9 ± 10.2	n. e.[a]
13	*i*-propylamino	6.42 ± 0.40	9.05 ± 1.15
14	*n*-propylamino	5.90 ± 0.42	9.58 ± 0.64
15	*n*-butylamino	6.62 ± 0.69	n. e.[a]
16	phenyl	n. e.[a]	n. e.[a]
17	anilino	5.38 ± 0.39	n. e.[a]
18	benzylamino	4.47 ± 0.31	n. e.[a]
19	phenylpropylamino	n. e.[a]	n. e.[a]
20	phenylbutylamino	n. e.[a]	n. e.[a]
21	2-pyridylmethylamino	3.40 ± 0.26	n. e.[a]
22	3-pyridylmethylamino	5.41 ± 0.46	20.7 ± 3.6
23	4-pyridylmethylamino	4.26 ± 0.18	n. e.[a]
24	2-hydroxyanilino	2.98 ± 0.36	n. e.[a]
25	3-hydroxyanilino	3.52 ± 0.45	4.08 ± 0.11
26	4-hydroxyanilino	4.54 ± 0.07	4.04 ± 0.11
27	4-cyanoanilino	6.75 ± 0.60	n. e.[a]
CsA		1.20 ± 0.03	2.95 ± 0.19

[a] n. e. = no effect.

2.3.5. *Reversal of ABCG2-mediated MDR*

While IC_{50} values give proof of their inhibitory power against ABCG2 – and therefore of their primary mode of action – half-maximal sensitization concentrations (EC_{50}) reveal the actual antiproliferative capability of the compounds. It can be considered as the most important value regarding the reversal of MDR, but has only very recently started to be addressed and highlighted properly [15–17,41–43]. In order to address this very important aspect, all herein reported compounds were evaluated in a MTT-based MDR reversal assay as reported earlier [15–17,41]. Using a dilution series of the ABCG2 substrate SN-38, different concentrations of the target compounds were added. The greater the MDR reversing property of the compound is, the lower is the concentration needed to shift the concentration-effect curve of SN-38 toward the left. This specifies that the amount of SN-38 required to half-maximally inhibit growth of ABCG2-overexpressing cells decreases. From plotting the

Table 3
Intrinsic toxicity of the 6-substituted 4-anilino-2-phenylpyrimidine derivatives obtained in a MTT-based cell viability assay using MDCK II BCRP and MDCK II cells as described earlier [15–17,41]. GI_{50} values are expressed as mean ± SEM of at least three independent experiments. The tr has been calculated by dividing the GI_{50} values of a compound by the corresponding IC_{50} value of the very same compound as shown in Table 1.

No	R	GI_{50} ± SEM [μM] MDCK II BCRP	GI_{50} ± SEM [μM] MDCK II	tr
12	methylamino	25.0 ± 3.7	34.1 ± 4.2	180
13	*i*-propylamino	5.06 ± 0.14	5.58 ± 0.11	6.68
14	*n*-propylamino	6.56 ± 0.20	8.34 ± 0.21	22.7
15	*n*-butylamino	6.08 ± 0.21	8.32 ± 0.35	12.2
16	phenyl	21.9 ± 1.6	25.1 ± 1.2	4.96
17	anilino	4.05 ± 0.31	4.95 ± 0.24	24.0
18	benzylamino	10.7 ± 0.8	4.19 ± 0.08	38.0
19	phenylpropylamino	3.64 ± 0.16	5.03 ± 0.11	38.4
20	phenylbutylamino	9.48 ± 0.05	10.6 ± 0.37	65.0
21	2-pyridylmethylamino	8.56 ± 0.51	9.44 ± 0.24	40.8
22	3-pyridylmethylamino	5.54 ± 0.09	7.47 ± 0.39	14.9
23	4-pyridylmethylamino	10.0 ± 0.1	10.7 ± 0.2	23.1
24	2-hydroxyanilino	4.61 ± 0.34	4.23 ± 0.13	20.7
25	3-hydroxyanilino	5.12 ± 0.07	5.24 ± 0.06	8.42
26	4-hydroxyanilino	5.15 ± 0.10	5.30 ± 0.06	13.4
27	4-cyanoanilino	7.78 ± 0.36	7.09 ± 0.29	58.7

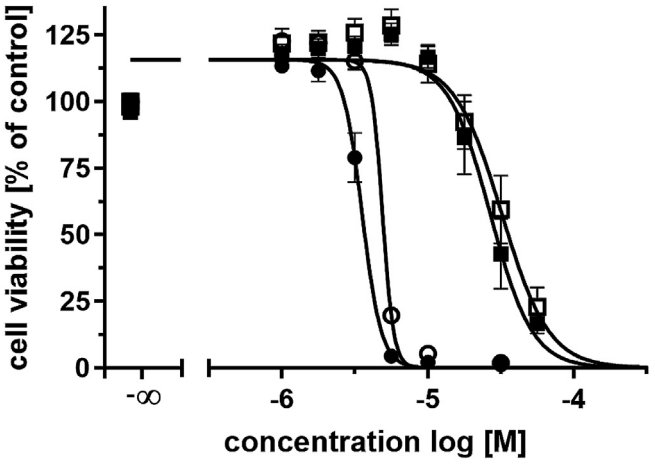

Fig. 6. MTT-based cell viability assays of compounds **12** (circles) and **19** (squares) using MDCK II BCRP (closed) and MDCK II (open) cells. While cell culture medium was taken as reference for full cell viability (100%), 10% DMSO defined 0% cell viability. Shown is mean ± SEM of at least three independent experiments.

resistance factors of each experiment against the concentration of the compound tested, the EC_{50} can be deduced. Table 5 gives the GI_{50} values obtained for all compounds at different concentrations, while Table 6 provides the EC_{50} values of these compounds. Fig. 7A and B shows the results obtained for the most potent reverser of ABCG2-mediated MDR within this manuscript, compound **14**. Strikingly, the obtained EC_{50} values of compounds **13**–**14** and **21** were in the low double-digit nanomolar concentration range. This gives these compounds an exceptional standing, as there have hardly been reported compounds with equal or superior efficacy [17,42].

2.3.6. Reversal of ABCB1- and ABCC1-mediated MDR

From this study, one compound (**24**) was found to be a moderately good dual ABCB1 and ABCG2 inhibitor and four compounds (**13**–**14**, **25**–**26**) were multitarget ABCB1, ABCC1, and ABCG2 inhibitors. Especially the latter finding is a rather unusual observation in literature [43]. Hence, these agents were assessed for their capability to reverse ABCB1- and ABCC1-mediated MDR applying a MTT-based cell viability assay as described earlier [15–17,40,41].

The intrinsic toxicity of compound **24** prevented test concentrations higher than 10 μM. Fig. 8A shows the GI_{50} values of the ABCB1 substrate daunorubicin dependent on the presence of either 0.5 μM, 1.0 μM, 5.0 μM, or 10 μM of compound **24**. Fig. 8B provides the resistance factors plotted against the tested concentrations of compound **24**. As can be seen from the plot, a tendency to a shift to lower resistance factors as a function of the used compound concentration could be determined. Compound **24** had an EC_{50} of 34.4 μM, however, considering its high intrinsic toxicity as outlined in Table 2, this value must be handled with care.

Unfortunately, the intrinsic toxicity and low potency of compounds **13**–**14** and **25**–**26** made it impossible to analyze their capability to reverse ABCB1- as well as ABCC1-mediated MDR (data not shown). Nevertheless, as the field of multitarget ABC transporter inhibitors emerged as a new potential therapeutic approach to target multidrug-resistant cancer cells [43,44,45,46], and the amount of potent broad-spectrum inhibitors is highly limited [11,15,27–35], the finding of these structures is of great interest

Table 4
Intrinsic toxicity of the 6-substituted 4-anilino-2-phenylpyrimidine derivatives obtained in a MTT-based cell viability assay using A2780/ADR, A2780, and H69AR cells as described earlier [15–17,40,41]. GI_{50} values are expressed as mean ± SEM of at least three independent experiments. The tr has been calculated by dividing the GI_{50} value of a compound by the corresponding IC_{50} value of the very same compound as shown in Table 2.

No	R	GI_{50} ± SEM [μM] A2780/ADR	tr	GI_{50} ± SEM [μM] A2780	GI_{50} ± SEM [μM] H69AR	tr
13	*i*-propylamino	8.09 ± 0.50	1.26	13.3 ± 0.6	21.4 ± 0.3	2.36
14	*n*-propylamino	12.3 ± 0.5	2.08	15.1 ± 0.4	23.0 ± 0.4	2.40
24	2-hydroxyanilino	9.96 ± 0.29	3.34	9.07 ± 0.34		
25	3-hydroxyanilino	5.91 ± 0.23	1.68	3.55 ± 0.31	11.0 ± 0.1	2.70
26	4-hydroxyanilino	9.21 ± 0.19	2.03	8.02 ± 0.31	13.7 ± 0.2	3.39

Table 5
Shift of GI_{50} values of SN-38 in the presence of different concentrations of the evaluated 6-substituted 4-anilino-2-phenylpyrimidines at 0.01 μM, 0.10 μM, and 1.00 μM. Data obtained using MDCK II BCRP as well as MDCK II cells. Shown is mean ± SEM of at least three independent experiments.

No	R	GI_{50} [μM] ± SEM resistant cells no compound	GI_{50} [μM] ± SEM resistant cells 0.01 μM compound	GI_{50} [μM] ± SEM resistant cells 0.10 μM compound	GI_{50} [μM] ± SEM resistant cells 1.00 μM compound	GI_{50} [μM] ± SEM sensitive cells no compound
12	methylamino	5.06 ± 0.38	3.62 ± 0.19	0.917 ± 0.026	0.407 ± 0.027	0.169 ± 0.021
13	*i*-propylamino	4.29 ± 0.26	2.93 ± 0.18	0.717 ± 0.045	0.314 ± 0.040	0.232 ± 0.044
14	*n*-propylamino	4.31 ± 0.30	2.78 ± 0.10	0.603 ± 0.035	0.334 ± 0.022	0.191 ± 0.021
15	*n*-butylamino	7.23 ± 1.48	5.81 ± 1.16	1.68 ± 0.44	0.731 ± 0.224	0.265 ± 0.098
16	phenyl	5.38 ± 0.40	4.44 ± 0.41	1.72 ± 0.16	0.367 ± 0.041	0.149 ± 0.015
17	anilino	5.09 ± 0.17	4.13 ± 0.16	1.64 ± 0.19	0.333 ± 0.024	0.187 ± 0.024
18	benzylamino	5.02 ± 0.47	3.62 ± 0.24	1.11 ± 0.05	0.421 ± 0.025	0.190 ± 0.018
19	phenylpropylamino	7.40 ± 1.92	6.55 ± 2.12	3.18 ± 1.00	0.727 ± 0.323	0.255 ± 0.140
20	phenylbutylamino	5.56 ± 0.38	4.84 ± 0.40	3.75 ± 0.34	0.494 ± 0.012	0.139 ± 0.014
21	2-pyridylmethylamino	4.56 ± 0.25	2.96 ± 0.08	0.616 ± 0.028	0.334 ± 0.029	0.231 ± 0.038
22	3-pyridylmethylamino	5.48 ± 0.26	4.66 ± 0.15	1.73 ± 0.05	0.415 ± 0.022	0.154 ± 0.014
23	4-pyridylmethylamino	4.67 ± 0.35	4.15 ± 0.25	2.09 ± 0.30	0.365 ± 0.030	0.256 ± 0.031
24	2-hydroxyanilino	4.88 ± 0.15	4.62 ± 0.27	3.07 ± 0.27	0.441 ± 0.028	0.158 ± 0.012
25	3-hydroxyanilino	4.74 ± 0.51	4.24 ± 0.97	3.28 ± 0.74	0.563 ± 0.110	0.265 ± 0.058
26	4-hydroxyanilino	3.85 ± 0.45	3.15 ± 0.43	2.57 ± 0.52	0.325 ± 0.023	0.195 ± 0.025
27	4-cyanoanilino	5.34 ± 0.64	5.12 ± 0.57	4.08 ± 0.51	0.563 ± 0.080	0.175 ± 0.028

Table 6
Quantification of the compound's ability to reverse ABCG2-mediated MDR determined with a MTT-based viability assay. The resistance factors derived from GI_{50} values from Table 5 were plotted against the corresponding concentration of the investigated compound. The nonlinear regression of the obtained curve gave the half-maximal reversal concentration (EC_{50}). Shown is mean ± SEM of at least three independent experiments.

No	R	EC_{50} [μM] ± SEM MDCK II BCRP
12	methylamino	0.0217 ± 0.0017
13	*i*-propylamino	0.0180 ± 0.0024
14	*n*-propylamino	0.0153 ± 0.0012
15	*n*-butylamino	0.0298 ± 0.0028
16	phenyl	0.0405 ± 0.0025
17	anilino	0.0435 ± 0.0024
18	benzylamino	0.0255 ± 0.0021
19	phenylpropylamino	0.0670 ± 0.0041
20	phenylbutylamino	0.187 ± 0.005
21	2-pyridylmethylamino	0.0155 ± 0.0006
22	3-pyridylmethylamino	0.0443 ± 0.0012
23	4-pyridylmethylamino	0.0725 ± 0.0094
24	2-hydroxyanilino	0.147 ± 0.008
25	3-hydroxyanilino	0.181 ± 0.023
26	4-hydroxyanilino	0.171 ± 0.024
27	4-cyanoanilino	0.231 ± 0.006

[43,47] and might help in the development of further, more potent, and less toxic therapeutics.

3. Binding mode analysis of 6-substituted 4-anilino-2-phenylpyrimidine derivatives

3.1. Classification of 6-substituted 4-anilino-2-phenylpyrimidine derivatives

Table 7 gives a summary of the obtained data of all compounds, which was taken in consideration for further validation of the developed computational model. For simplicity, positive and negative characteristics of the compounds were marked with green or red, respectively. The IC_{50} and I_{max} values were taken from Table 1. The selectivity ratios (sr) were calculated from values of Tables 1 and 2 The therapeutic ratios (tr) were assembled from Table 3. The EC_{50} values were compiled from Table 4, and the maximal degree of sensitization (°s) was calculated from the values of Table 5 as previously reported [15]. The cut-off values to determine preferable (green) or less preferable (red) properties were set according to critical markers. Regarding ABCG2 inhibition (IC_{50}), 0.25 μM was chosen as this represents superiority compared to the gold standard for ABCG2 inhibition, compound **28**. The I_{max} cut-off value was set at 75% as previously reported [15]. Selectivity and therapeutic ratios were considered to be preferable at ≥10. Since double-digit nanomolar sensitizers were reported before [17,37,42], a fairly low EC_{50} of 20 nM was chosen to classify the compounds. Finally, the maximal degree of sensitization was considered ≥50% to be preferable. As can be seen from Table 7, compound **21** was found as the only representative that fulfilled the requirements regarding the defined positive compound characteristics. Hence, it was used first to evaluate the mode of inhibition regarding the BCRP-mediated Hoechst 33342 transport, and second to validate the computational model by docking studies as reported earlier [17,26].

3.2. Determination of mode of inhibition of compound 21

As pyrimidines were shown before to inhibit ABCG2-mediated Hoechst 33342 transport competitively [17,26], compound **21** was evaluated to confirm the same mode of action as basis for ongoing *in silico* experiments. The Lineweaver-Burk analysis as depicted in Fig. 9 underpins the expected mode of competitive inhibition of the compound class of the 6-substituted 4-anilino-2-phenylpyrimidine derivatives in general and compound **21** in particular.

3.3. Molecular docking studies of compound 21

In order to visualize the hypothesis of the new binding (sub) pocket in the binding site of ABCG2 we took compound **21** for ongoing *in silico* experiments. As shown in Fig. 10, the binding pose of **21** was similarly oriented as compound **8** [17]. The pyrimidine scaffold formed hydrogen bond interactions with Asn387 and Asn391, the 4-cyanophenyl group at position 2 was oriented in the hydrophobic pocket formed by Val129, Val130, Met131, Gly132, Val178, Thr180 and Val450 and the cyano group formed strong electrostatic interaction with Arg191, while the phenyl substituent at position 4 was positioned in a pocket formed by Leu388, Leu447 and Asp477. The methyl-2-pyridyl substituent connected by an amino linker at position 6 of the pyrimidine scaffold oriented in the identified (sub)pocket and possibly formed interactions with Phe182 and Glu446 located at a distance of 3.2 Å and 3.6 Å,

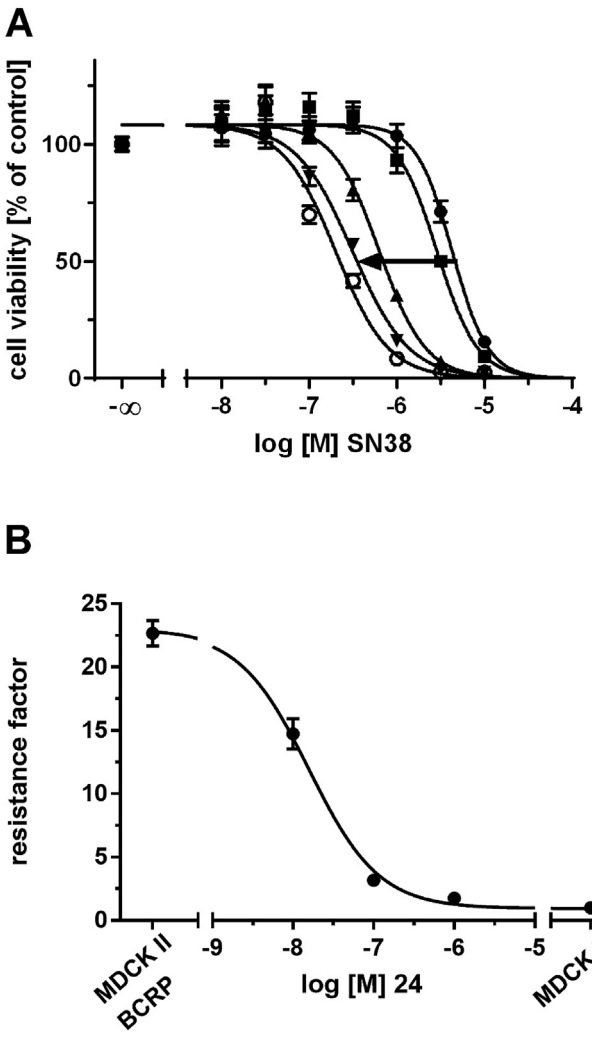

Fig. 7. Reversal of ABCG2-mediated MDR by compound **14** determined with a MTT-based cell viability assay. (A) Sensitization of ABCG2-overexpressing MDCK II BCRP cells with regard to SN-38. Compound **14** was used at concentrations of 0 μM (●), 0.010 μM (■), 0.100 μM (▲), as well as 1.000 μM (▼), and was compared to the wild type cell line without compound addition (○). Shown is mean ± SEM of at least three independent experiments. (B) Plotted resistance factors derived from GI_{50} values from Table 5 against applied concentrations of compound **14**. Nonlinear regression of the obtained curve resulted in the half-maximal reversal concentration (EC_{50}) of 15.3 ± 1.2 nM.

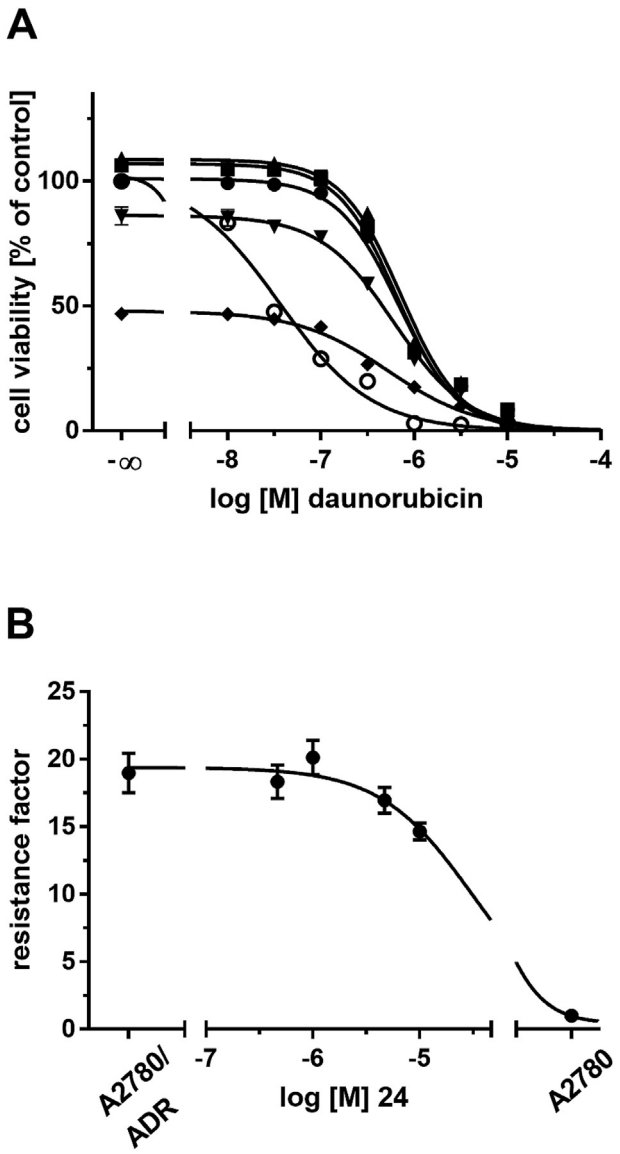

Fig. 8. Reversal of ABCB1-mediated MDR by compound **24** determined with a MTT-based cell viability assay. (A) Sensitization of ABCB1-overexpressing A2780/ADR cells with regard to daunorubicin. Compound **24** was used at concentrations of 0 μM (●), 0.5 μM (■), 1.0 μM (▲), 5.0 μM (▼), as well as 10.0 μM (◆), and was compared to the wild type cell line without compound supplementation (○). Shown is mean ± SEM of at least three independent experiments. (B) Plotted resistance factors derived from GI_{50} values from (A) against applied concentrations of compound **24**. Nonlinear regression and extrapolation of the obtained curve resulted in the half-maximal reversal concentration (EC_{50}) of 34.4 ± 4.9 μM.

respectively. The amino linker between might introduce flexibility for the different substitutions at position 6. The hypothesis is supported by compound **16**, where a phenyl substitution resulted in severe loss of activity against ABCG2 possibly due to steric clashes in the binding pocket. Furthermore, the substituted aromatic residues, in particular at position 2, favored the interaction with the amino acid residues in the binding (sub)pocket. Additionally, it opened up the possibility for further exploration of the (sub)pocket with different substitutions to improve the activity and properties of ABCG2 inhibitors in general.

4. Conclusions

4-Anilino-6-methyl-2-phenylpyrimidines were discovered as highly potent inhibitors of ABCG2 [17], with an efficacy regarding reversal of ABCG2-mediated MDR that has barely been reported before [17,23,42]. Molecular docking studies revealed a binding (sub)pocket which was explored as part of the current study. The herein presented 6-substituted 4-anilino-2-phenylpyrimidines have three major properties: (i) they are like their parent compounds highly potent regarding ABCG2 inhibition, which is reflected in seven compounds (**12**, **17**, **19**–**21**, **24**, **27**) having IC_{50} values of less than 250 nM – making them significantly more potent than the gold standard compound **28**; (ii) similar to their parent compounds, their efficacy regarding reversal of ABCG2-mediated MDR is some of the highest reported in the literature [17,23,42]. This accounts especially for compounds **13**–**14**, and **21** with EC_{50} values below 20 nM; (iii) due to their 6-substitution, these compounds inherited exceptional cell toxicity, with single-digit GI_{50} values for most of the evaluated compounds – independent from the used cell lines. However, as their inhibitory

Table 7
Summary of obtained biological results of tested 6-substituted 4-anilino-2-phenylpyrimidine derivatives as taken and/or calculated from Tables 1–6 Positive and negative compound characteristics are depicted in green and red, respectively.

No	R	IC_{50}[a]	I_{max}[b]	sr_{ABCB1}[c]	sr_{ABCC1}[d]	tr[e]	EC_{50}[f]	°s[g]
12	methylamino	0.141	68	184	n. e.[h]	180	0.0217	41
13	*i*-propylamino	0.763	101	8	12	6.68	0.0180	74
14	*n*-propylamino	0.293	89	20	33	22.7	0.0153	58
15	*n*-butylamino	0.500	73	13	n. e.[h]	12.2	0.0298	36
16	phenyl	4.41	81[i]	n. e.[h]	n. e.[h]	4.96	0.0405	40
17	anilino	0.169	84	32	n. e.[h]	24.0	0.0435	58
18	benzylamino	0.283	99	16	n. e.[h]	38.0	0.0255	46
19	phenylpropylamino	0.0960	61	n. e.[h]	n. e.[h]	38.4	0.0670	35
20	phenylbutylamino	0.147	61	n. e.[h]	n. e.[h]	65.0	0.187	29
21	2-pyridylmethylamino	0.210	88	16	n. e.[h]	40.8	0.0155	70
22	3-pyridylmethylamino	0.373	91	15	55	14.9	0.0443	36
23	4-pyridylmethylamino	0.435	78	10	n. e.[h]	23.1	0.0725	72
24	2-hydroxyanilino	0.223	86	13	n. e.[h]	20.7	0.147	36
25	3-hydroxyanilino	0.608	66	6	7	8.42	0.181	47
26	4-hydroxyanilino	0.387	76	12	10	13.4	0.171	62
27	4-cyanoanilino	0.133	60	51	n. e.[h]	58.7	0.231	30

a = the half maximal-inhibition concentration (IC50) values were taken from Table 1.
b = the maximal inhibition (Imax) values were taken from Table 1.
c = the selectivity ratios over ABCB1 were calculated by taking the IC50 (ABCB1) of the compounds from Table 2 divided by the IC50 (ABCG2) values of the corresponding compounds from Table 1.
d = the selectivity ratios over ABCC1 were calculated by taking the IC50 (ABCC1) of the compounds from Table 2 divided by the IC50 (ABCG2) values of the corresponding compounds from Table 1.
e = the therapeutic ratios (tr) were taken from Table 3.
f = the half-maximal sensitization concentrations (EC50) were obtained from Table 4.
g = the maximal degree of sensitization (°s) was calculated as reported before [15] from the potentiation factor of the compound at 1 μM divided by the resistance factor of the resistant cell line without treatment. The potentiation factor was calculated taking the GI50 value of the untreated resistant cells (Table 5) divided by the GI50 values of the resistant cells treated with 1 μM of the compound (Table 5). The resistance factors were calculated by taking the GI50 values of the resistant cells without treatment (Table 5) divided by the GI50 values of the sensitive cell line (Table 5).
h = n. e. = no effect.
i = Imax at highest tested concentration.

power and efficacy were determined in a much lower concentration range, it can be concluded that the compounds exerted their reversal of ABCG2-mediated MDR due to ABCG2 inhibition. Nevertheless, their intrinsic toxicity is an undesired side effect, making these compounds generally less applicable for anticancer therapy.

The most significant finding of this work is that the previously discovered (sub)pocket [17] could be used to engage the herein presented compound **21** by strong interactions with its molecular target, human ABCG2. To our best knowledge, this is the very first time that a structure-based drug design approach successfully discovered new and highly potent ABCG2 inhibitors and elucidated in parallel the drug-target interaction.

Interestingly, the herein evaluated compounds contained five multitarget ABCB1, ABCC1, and ABCG2 inhibitors, four of them exerting their inhibitory power against the three stated transporters at least in the single-digit micromolar concentration range. Until now, less than 140 compounds have been reported with this ability. Among these, only around 50 have been found to exert their inhibitory power against ABCB1, ABCC1, and ABCG2 below 10 μM [11,15–17,27–36,42,48–55] Hence, the sole discovery of compounds **13**–**14** and **25**–**26** is very important for ongoing research to understand the function of ABC transporters in general and the necessities for inhibition of the particular representatives, as these compounds belong to the 50 most potent triple ABCB1, ABCC1, and ABCG2 inhibitors ever reported. Strikingly, compounds **25**–**26** belong even to the 22 most potent multitarget inhibitors that have IC_{50} values against ABCB1, ABCC1, and ABCG2 $\leq$5 μM [11,15,27–36]. As broad-spectrum reversers of ABCB1-, ABCC1-, and ABCG2-mediated MDR have barely been reported [10,13–24], this discovery might be of great importance in the field of multitarget ABC transporter inhibition [43,47].

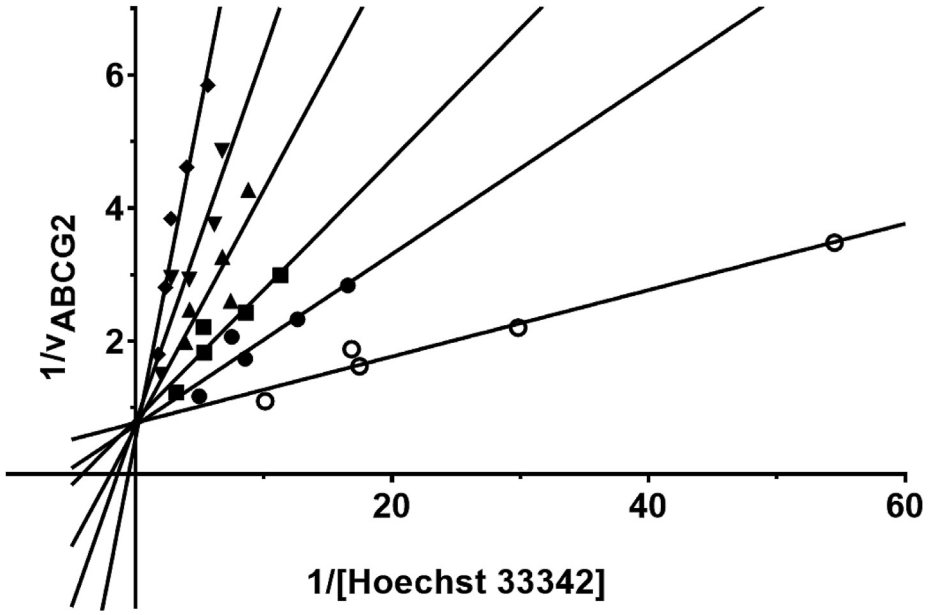

Fig. 9. Lineweaver-Burk plot of compound **21** using ABCG2-overexpressing MDCK II BCRP cells. Hoechst 33342 was used at 0.3, 0.4, 0.5, 0.6, 0.7, and 1.0 μM. Compound **21** was used at concentrations of 0 μM (○), 0.00560 μM (●), 0.0100 μM (■), 0.0178 μM (▲), 0.0316 μM (▼), and 0.0562 (◆). Depicted is a representative experiment out of three independent experiments.

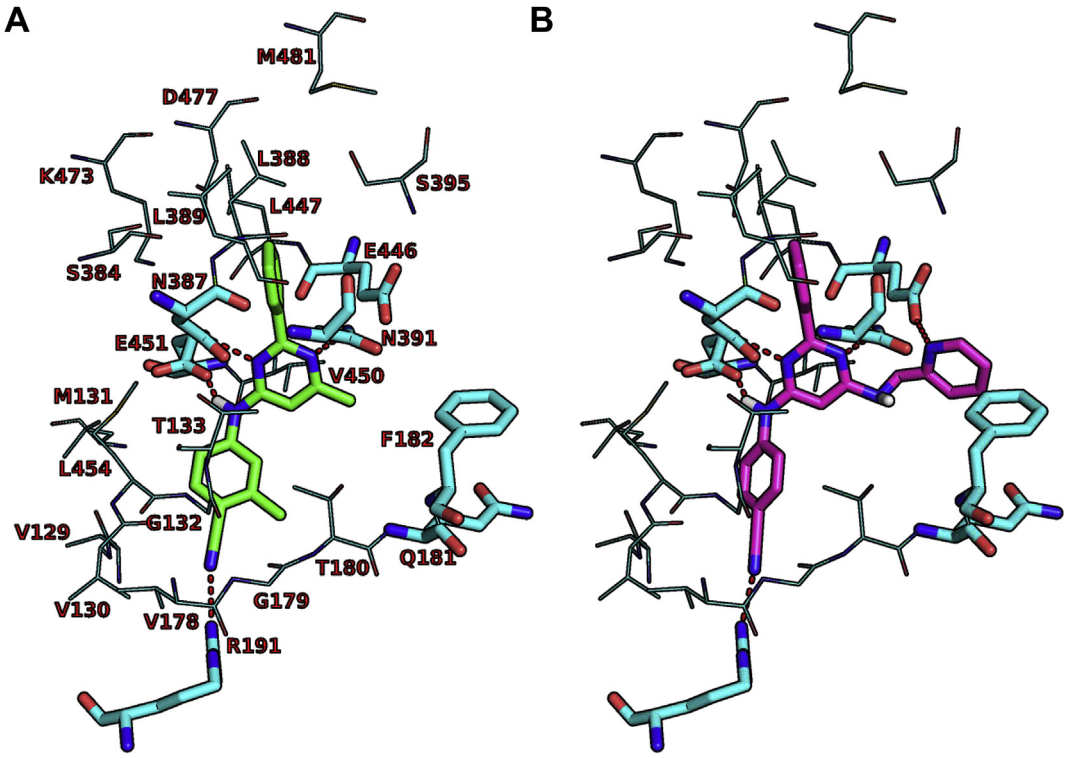

Fig. 10. The docked pose of **8** (carbon colored green) and **21** (carbon colored magenta) as observed in the binding pocket of human ABCG2 (PDB ID: 6FFC). The amino acids in the binding pocket are shown as line representation and in particular the important residues that possibly form interaction with the compounds are indicated in stick representation. The interactions with the compounds are shown in red dashed lines. Oxygen atoms are colored in red, nitrogen atoms in blue, and polar hydrogen atoms are colored in white. (For interpretation of the references to color in this figure legend, the reader is referred to the Web version of this article.)

5. Experimental section

5.1. Molecular docking

The human ABCG2 transporter was crystallized using cryo-electron microscopy (cryo-EM) in complex with the fumitremorgin *C*-related inhibitor, MZ29 (PDB ID: 6FFC) was downloaded from Research Collaboratory for Structural Bioinformatics Protein Data Bank (PDB) [23]. As an initial step, the structure was prepared and protonated using the protein structure preparation and Protonate3D modules implemented in Molecular Operating Environment (MOE) 2018.01, respectively [56]. Then the receptor structure of the human ABCG2 was applied for flexible ligand docking using LeadIT from BioSolveIT, GmbH Germany [57]. During the docking simulations, the ligands were fully flexible while the residues of the receptor were treated as rigid. For the docking calculations, the binding site of the receptor was defined in 20 Å spacing of the amino acid residues centered based on the cocrystallized ligand, MZ29. Then the selected compounds were docked with default parameters and predicted the binding pose using the FlexX module implemented in LeadIT [58]. From the resulted binding poses, the top 100 highest scoring docked poses were selected for the analysis. Then the docked pose having the lowest binding free energy for interactions was visualized and selected as the putative binding mode of the compound using MOE2018.01 [56].

5.2. Chemistry

5.2.1. Materials

Chemicals were purchased from Acros Organics (Geel, Belgium), Alfa Aesar (Karlsruhe, Germany), SigmaAldrich (Steinheim, Germany), Carl Roth GmbH (Karlsruhe, Germany), Calbiochem (San Diego, CA, USA), Frontier Scientific Inc. (Logan, UT, USA), or Merck (Darmstadt, Germany). Microwave reactions were performed in 10 mL vials with a CEM Discover SP (CEM GmbH, Kamp-Lintfort, Germany). The reaction progress was monitored by thin layer chromatography (TLC) using an aluminum plate coated with silica gel 60 F254 (Merck Millipore, Billerica, MA, USA). Dichloromethane/methanol and ethyl acetate/petroleum ether (40–60 °C) were used as eluents. The identity of the compounds was confirmed by NMR. ^{1}H- and ^{13}C spectra were obtained on Bruker Advance 500 MHz (500/126 MHz) or Bruker Advance 600 MHz (600/151 MHz). The chemical shifts (δ) are expressed in ppm. For the assignment of some ^{13}C signals, attached proton test (APT) was used. Multiplicity of the signals is indicated as singlet (s), doublet (d), triplet (t), quartet (q), quintet (p) and multiplet (m). Coupling constants J are given in Hz. The purity and molecular mass of compounds were determined by LC-MS (Applied Biosystems API 2000 LC-MS/MS, HPLC Agilent 1100). Krebs-HEPES-buffer [KHB; $CaCl_2$ (1.3 mM), D-glucose monohydrate (11.7 mM), HEPES (10.0 mM), KCl (4.7 mM), KH_2PO_4 (1.2 mM), $MgSO_4$ (1.2 mM), NaCl (118.6 mM), $NaHCO_3$ (4.2 mM), and NaOH (adjusting to pH = 7.4) was filtered sterile and used for dilutions. The reference compounds cyclosporine A (ABCB1) and Ko143 [(3*S*,6*S*,12a*S*)-1,2,3,4,6,7,12,12a-octahydro-9-methoxy-6-(2-methylpropyl)-1,4-dioxopyrazino[1′,2′:1,6]pyrido[3,4-*b*]indole-3-propanoic acid 1,1-dimethylethylester; compound **28**; ABCG2] were delivered by Tocris Bioscience (Bristol, IO, USA). Calcein AM (ABCC1 and ABCB1) and pheophorbide A (ABCG2) were purchased from Calbiochem [EMD Chemicals (San Diego, CA, USA] and Frontier Scientific Inc. (Logan, UT, USA), respectively. Daunorubicin was delivered by Sigma (Oakville, ON, Canada). SN-38 was supplied by Tocris Bioscience (Bristol, IO, USA). Other chemicals were purchased from Carl Roth GmbH (Karlsruhe, Germany), Merck KgaA (Darmstadt, Germany), Th. Geyer GmbH Co KG (Renningen, Germany) and Sigma-Aldrich Chemie GmbH (Steinheim, Germany). Storage of the used compounds (10 mM stock solution) was performed in dimethylsulfoxide (DMSO) at −20 °C. Krebs-HEPES buffer [KHB; $CaCl_2$ (1.3 mM)], D-glucose monohydrate (11.7 mM), HEPES (N-2-hydroxyethylpiperazin-N′-2-ethansulfonic acid; 10.0 mM), KCl (4.7 mM), KH_2PO_4 (1.2 mM) $MgSO_4$ (1.2 mM) NaCl (118.6 mM) $NaHCO_3$ (4.2 mM), and NaOH (adjusting to pH = 7.4) were used for dilutions. Before use, KHB was sterile filtered with membrane filters (Whatman FP 30/0.2 μM CA-S filter units, GE Healthcare UK Limited, Buckinghamshire, UK) using a Braun Injekt 20 mL syringe (ALMO-Erzeugnisse, Erwin Busch GmbH, Bad Arolsen, Germany) and stored in cellstar 50 mL tubes (Greiner Bio-One, Frickenhausen, Germany).

5.2.2. Synthesis

*5.2.2.1. Preparation of 2-phenylpyrimidine-4,6-diol (**9**).* 5.56 g (241.7 mmol) sodium were dissolved in 200 ml ethanol to yield sodium ethoxide solution. Subsequently, 12.18 g (66 mmol) benzamidine hydrochloride hydrate and 11.79 g (89 mmol) ethyl dimethyl malonate were added into sodium ethoxide solution respectively. The resulting mixture was heated to reflux overnight and cooled down to room temperature. After solvent was removed under reduced pressure, 50 ml of water were added to the solid and the mixture was acidified with concentrated HCl to pH 5–6. The formed precipitate was vacuum filtered and washed with water three times. Finally, the obtained crude residue was recrystallized from DMF/H_2O to give 2-phenylpyrimidine-4,6-diol as orange solid (5.8 g; 46.7%).^{1}H NMR (500 MHz, DMSO-d_6) δ: 11.80 (s, 2H), 8.11–8.07 (m, 2H), 7.60–7.56 (m, 1H), 7.54–7.50 (m, 2H), 5.35 (s, 1H). ^{13}C NMR APT (126 MHz, DMSO) δ: 131.81, 128.69, 127.87, 88.46.

*5.2.2.2. Preparation of 4,6-dichloro-2-phenylpyrimidine (**10**).* 5.8 g (30.8 mmol) 2-phenylpyrimidine-4,6-diol was added to 20 ml $POCl_3$. The solution was refluxed until the reaction was complete. Excess $POCl_3$ was removed under reduced pressure. The oily residue was transferred onto crushed ice portion by portion while keeping the temperature of solution below 10 °C. Ethyl acetate was used to extract products 3 times. The organic layer was washed with saturated $NaHCO_3$, saturated NaCl solution and dried over magnesium sulfate. After filtration, ethyl acetate was removed under reduced pressure. Final purification was performed by column chromatography with DCM/MeOH = 50:1 as eluent to yield white needle crystals (yield: 4.1 g; 59.4%). ^{1}H NMR (600 MHz, $CDCl_3$) δ: 8.44 (d, J = 7.9 Hz, 2H), 7.56–7.48 (m, 3H), 7.28 (s, 1H). ^{13}C NMR (126 MHz, $CDCl_3$) δ: 165.91, 162.18, 135.02, 132.40, 129.02, 128.88, 118.91.

*5.2.2.3. Preparation of 4-((6-chloro-2-phenylpyrimidin-4-yl)amino) benzonitrile (**11**).* 3.04 g (13.5 mmol) 4,6-dichloro-2-phenylpyrimidine was added to 30 ml isopropanol and this mixture was refluxed until all 4,6-dichloro-2-phenylpyrimidine was dissolved. 1.57 g (13.3 mmol) 4-cyanoaniline was dissolved in 30 ml isopropanol and this solution was added dropwise to refluxed 4,6-dichloro-2-phenylpyrimidine solution. If reaction did not initiate, 0.1 equivalent of conc. HCl was added as catalyst. The precipitate was filtered off and washed with saturated sodium bicarbonate solution 3 times followed by distilled water 3 times. Further purification was performed by column chromatography with ethyl acetate/petroleum ether (40–60 °C) = 1:2 as eluent, yellow solid (3.6 g, 88.2%).^{1}H NMR (500 MHz, DMSO-d_6) δ: 10.34 (s, 1H), 8.32–8.29 (m, 2H), 7.97–7.94 (m, 2H), 7.87–7.84 (m, 2H), 7.58–7.53 (m, 3H), 6.85 (s, 1H). ^{13}C NMR (126 MHz, DMSO) δ: 163.70, 160.98, 158.82, 143.56, 136.07, 133.31, 131.43, 128.72, 127.92, 119.67, 119.10, 104.52, 104.15. LC-MS (m/z) calcd. for $C_{17}H_{11}ClN_4$

$[M+1]^+$: 307.07, Found: 307.2, Purity: 97.9%.

*5.2.2.4. General procedure for the preparation of 4-anilino-2-phenylpyrimidine derivatives (**12**–**27**)*

5.2.2.4.1. Method A. A mixture of 1 equivalent 4-((6-chloro-2-phenylpyrimidin-4-yl)amino)benzonitrile, 10–20 equivalent of amine in 0.5 ml isopropanol was heated to 120 °C in microwave for 30 min. Further purification for certain compounds was performed by column chromatography with ethyl acetate/petroleum ether (40–60 °C) = 1:2 as eluent.

5.2.2.4.2. Method B. To a three necked round-bottom flask were added 112 mg 4-((6-chloro-2-phenylpyrimidin-4-yl)amino)benzonitrile (0.37 mmol), 50 mg phenylboronic acid (0.41 mmol) and 8 ml Dioxane/2M K_2CO_3 = 3:1. The mixture was degassed by vacuum/argon cycle three times. Catalyst 10 mg Pd(t-Bu_3P)$_2$ (0.02 mmol) was added and the mixture was degassed twice more. The mixture was heated to 85 °C for 7 h until TLC confirmed the completion of the reaction and cooled to ambient temperature. Afterward, the slurry was extracted with saturated $NaHCO_3$/ethyl acetate 3 times. The collected ethyl acetate solution was dried over magnesium sulfate and concentrated under reduced pressure. Further purification was performed by recrystallization from ethyl acetate/n-hexane.

5.2.2.4.3. Method C. A mixture of 1 equivalent 4-((6-chloro-2-phenylpyrimidin-4-yl)amino)benzonitrile, 10–15 equivalent of substituted aniline in 3 ml isopropanol and 0.1 equivalent conc. HCl was heated to 110 °C in microwave for 30 min. The precipitate was filtered off and washed with saturated sodium bicarbonate solution 3 times followed by distilled water 3 times. Further purification was performed by column chromatography with ethyl acetate/petroleum ether (40–60 °C) = 1:2 as eluent.

*5.2.2.5. 4-((6-(methylamino)-2-phenylpyrimidin-4-yl)amino)benzonitrile (**12**).* The title compound was synthesized from 4-((6-chloro-2-phenylpyrimidin-4-yl)amino)benzonitrile (136 mg, 0.44 mmol), methylamine hydrochloride (306 mg, 4.53 mmol) and *N*,*N*-diisopropylethylamine (0.8 ml, 4.48 mmol) as described in the general procedure of method A. Yellow solid (20.7 mg, 15.5%). ^{1}H NMR (500 MHz, DMSO-d_6) δ: 9.57 (s, 1H), 8.32 (dd, J = 3.1, 6.6 Hz, 2H), 7.91 (d, J = 8.6 Hz, 2H), 7.75–7.68 (m, 2H), 7.51–7.40 (m, 3H), 7.07 (s, 1H), 5.80 (s, 1H), 2.87 (s, 3H). ^{13}C NMR (126 MHz, DMSO) δ: 163.78, 162.18, 159.71, 145.64, 138.29, 133.06, 130.03, 128.19, 127.55, 119.59, 118.26, 101.58, 27.35. LC-MS (m/z) calcd. for $C_{18}H_{15}N_5$ $[M+1]^+$: 302.13, Found: 302.0, Purity: 98.3%.

*5.2.2.6. 4-((6-(isopropylamino)-2-phenylpyrimidin-4-yl)amino)benzonitrile (**13**).* The title compound was synthesized from 4-((6-chloro-2-phenylpyrimidin-4-yl)amino)benzonitrile (141 mg, 0.46 mmol) and isopropylamine (880 mg, 14.89 mmol) as described in the general procedure of method A. Yellow solid (100.3 mg, 66.1%).

^{1}H NMR (500 MHz, DMSO-d_6) δ: 9.54 (s, 1H), 8.32–8.29 (m, 2H), 7.89 (d, J = 8.7 Hz, 2H), 7.74–7.71 (m, 2H), 7.50–7.46 (m, 3H), 6.99 (d, J = 7.4 Hz, 1H), 5.81 (s, 1H), 1.21 (d, J = 6.5 Hz, 6H). ^{13}C NMR (126 MHz, DMSO) δ: 162.49, 162.25, 145.73, 138.42, 133.07, 130.02, 128.22, 127.53, 119.64, 118.25, 101.50, 59.71, 41.74, 22.50, 14.06. LC-MS (m/z) calcd. for $C_{20}H_{19}N_5$ $[M+1]^+$: 330.16, Found: 330.1, Purity: 99.0%.

*5.2.2.7. 4-((2-phenyl-6-(propylamino)pyrimidin-4-yl)amino)benzonitrile (**14**).* The title compound was synthesized from 4-((6-chloro-2-phenylpyrimidin-4-yl)amino)benzonitrile (168 mg, 0.55 mmol) and 1-propylamine (308 mg, 5.22 mmol) as described in the general procedure of method A. White solid (126.4 mg, 69.9%). ^{1}H NMR (500 MHz, DMSO-d_6) δ: 9.54 (s, 1H), 8.33–8.28 (m, 2H), 7.90 (d, J = 8.9 Hz, 2H), 7.75–7.70 (m, 2H), 7.51–7.45 (m, 3H), 7.14 (s, 1H), 5.83 (s, 1H), 1.61 (h, J = 7.4 Hz, 2H), 0.95 (t, J = 7.4 Hz, 3H). ^{13}C NMR (126 MHz, DMSO) δ: 163.25, 162.20, 145.68, 138.36, 133.05, 130.00, 128.19, 127.52, 119.59, 118.24, 101.52, 42.20, 22.15, 11.52. LC-MS (m/z) calcd. for $C_{20}H_{19}N_5$ $[M+1]^+$: 330.16, Found: 330.1, Purity: 99.3%.

*5.2.2.8. 4-((6-(butylamino)-2-phenylpyrimidin-4-yl)amino)benzonitrile (**15**).* The title compound was synthesized from 4-((6-chloro-2-phenylpyrimidin-4-yl)amino)benzonitrile (125 mg, 0.41 mmol) and 1-butylamine (390 mg, 5.33 mmol) as described in the general procedure of method A. Brown solid (66.5 mg, 47.4%). ^{1}H NMR (500 MHz, DMSO-d_6) δ: 9.55 (s, 1H), 8.32–8.29 (m, 2H), 7.90 (d, J = 8.4 Hz, 2H), 7.75–7.71 (m, 2H), 7.51–7.46 (m, 3H), 7.14 (s, 1H), 5.82 (s, 1H), 1.60–1.54 (m, 2H), 1.39 (q, J = 7.4 Hz, 2H), 0.93 (t, J = 7.4 Hz, 3H). ^{13}C NMR (126 MHz, DMSO) δ: 163.25, 162.22, 145.71, 138.39, 133.09, 130.05, 128.23, 127.54, 119.64, 118.27, 101.53, 19.68, 13.73. LC-MS (m/z) calcd. for $C_{21}H_{21}N_5$ $[M+1]^+$: 344.18, Found: 344.1, Purity: 98.9%.

*5.2.2.9. 4-((2,6-diphenylpyrimidin-4-yl)amino)benzonitrile (**16**).* The title compound was synthesized as described in the general procedure of method B. Yellow solid (63.0 mg, 49.6%). ^{1}H NMR (500 MHz, DMSO-d_6) δ: 10.26 (s, 1H), 8.51–8.48 (m, 2H), 8.21–8.18 (m, 2H), 8.07–8.04 (m, 2H), 7.87–7.84 (m, 2H), 7.62–7.55 (m, 6H), 7.29 (s, 1H). ^{13}C NMR (126 MHz, DMSO) δ: 163.02, 162.22, 161.01, 144.44, 137.68, 136.81, 133.31, 130.74, 130.63, 128.98, 128.61, 127.87, 126.61, 119.34, 119.16, 103.24, 101.47. LC-MS (m/z) calcd. for $C_{23}H_{16}N_4$ $[M+1]^+$: 349.14, Found: 349.0, Purity: 97.1%.

*5.2.2.10. 4-((2-phenyl-6-(phenylamino)pyrimidin-4-yl)amino)benzonitrile (**17**).* The title compound was synthesized from 4-((6-chloro-2-phenylpyrimidin-4-yl)amino)benzonitrile (127 mg, 0.41 mmol) and aniline (508 mg, 5.46 mmol) as described in the general procedure of method C. White solid (47.6 mg, 31.8%). ^{1}H NMR (500 MHz, DMSO-d_6) δ: 9.77 (s, 1H), 9.37 (s, 1H), 8.36–8.32 (m, 2H), 7.95–7.91 (m, 2H), 7.79–7.75 (m, 2H), 7.69–7.64 (m, 2H), 7.56–7.50 (m, 3H), 7.41–7.35 (m, 2H), 7.04 (tt, J = 1.1, 7.3 Hz, 1H), 6.23 (s, 1H). ^{13}C NMR (126 MHz, DMSO) δ: 162.61, 161.09, 160.17, 145.25, 140.23, 138.03, 133.13, 130.37, 128.79, 128.42, 127.61, 122.09, 120.08, 119.49, 118.59, 102.11, 86.90. LC-MS (m/z) calcd. for $C_{23}H_{17}N_5$ $[M+1]^+$: 364.15, Found: 364.0, Purity: 99.1%.

*5.2.2.11. 4-((6-(nenzylamino)-2-phenylpyrimidin-4-yl)amino)benzonitrile (**18**).* The title compound was synthesized from 4-((6-chloro-2-phenylpyrimidin-4-yl)amino)benzonitrile (76 mg, 0.25 mmol) and benzylamine (270 mg, 2.52 mmol) as described in the general procedure of method A. Brown solid (25.3 mg, 27.3%). ^{1}H NMR (500 MHz, DMSO-d_6) δ: 9.58 (s, 1H), 8.30 (dd, J = 3.0, 6.7 Hz, 2H), 7.88 (d, J = 8.8 Hz, 2H), 7.75–7.70 (m, 3H), 7.48 (dd, J = 1.9, 5.0 Hz, 3H), 7.40–7.37 (m, 2H), 7.34 (t, J = 7.6 Hz, 2H), 7.24 (t, J = 7.3 Hz, 1H), 5.86 (s, 1H), 4.60 (s, 2H). ^{13}C NMR (126 MHz, DMSO) δ: 163.19, 162.25, 159.77, 145.58, 140.13, 138.23, 133.08, 130.12, 128.31, 128.25, 127.57, 127.17, 126.70, 119.60, 118.32, 101.65, 43.79. LC-MS (m/z) calcd. for $C_{24}H_{19}N_5$ $[M+1]^+$: 378.16, Found: 378.3, Purity: 96.7%.

*5.2.2.12. 4-((2-phenyl-6-((3-phenylpropyl)amino)pyrimidin-4-yl)amino)benzonitrile (**19**).* The title compound was synthesized from 4-((6-chloro-2-phenylpyrimidin-4-yl)amino)benzonitrile (86 mg, 0.28 mmol) and 3-phenylpropylamine (759 mg, 5.61 mmol) as described in the general procedure of method A. White solid (70.3 mg, 61.9%). ^{1}H NMR (500 MHz, DMSO-d_6) δ: 9.54 (s, 1H), 8.30–8.25 (m, 2H), 7.90 (d, J = 8.6 Hz, 2H), 7.75–7.71 (m, 2H), 7.50–7.46 (m, 3H), 7.32–7.17 (m, 6H), 5.83 (s, 1H), 3.36 (d,

J = 18.3 Hz, 0H), 2.69 (t, J = 7.6 Hz, 2H), 1.90 (p, J = 7.3 Hz, 2H). ^{13}C NMR (126 MHz, DMSO) δ: 163.21, 162.19, 159.55, 145.66, 141.72, 138.31, 133.05, 130.02, 128.28, 128.22, 128.18, 127.53, 125.67, 119.59, 118.27, 101.55, 32.62, 30.73. LC-MS (m/z) calcd. for $C_{26}H_{23}N_5$ $[M+1]^+$: 406.20, Found: 406.3, Purity: 98.0%.

*5.2.2.13. 4-((2-phenyl-6-((4-phenylbutyl)amino)pyrimidin-4-yl) amino)benzonitrile (**20**).* The title compound was synthesized from 4-((6-chloro-2-phenylpyrimidin-4-yl)amino)benzonitrile (130 mg, 0.42 mmol) and 4-phenylbutylamine (522 mg, 3.50 mmol) as described in the general procedure of method A. Pale brown solid (76.8 mg, 43.3%). ^{1}H NMR (500 MHz, DMSO-d_6) δ: 9.55 (s, 1H), 8.32−8.28 (m, 2H), 7.89 (d, J = 8.4 Hz, 2H), 7.75−7.71 (m, 2H), 7.50−7.45 (m, 3H), 7.26 (t, J = 7.5 Hz, 2H), 7.20 (d, J = 6.8 Hz, 2H), 7.18−7.14 (m, 2H), 5.82 (s, 1H), 2.64 (t, J = 7.5 Hz, 2H), 1.71−1.64 (m, 2H), 1.64−1.57 (m, 2H). ^{13}C NMR (126 MHz, DMSO) δ: 163.23, 162.24, 145.70, 142.11, 138.38, 133.09, 130.05, 128.25, 128.22, 128.18, 127.56, 125.61, 119.64, 118.27, 101.53, 55.99, 34.84, 28.46, 18.52. LC-MS (m/z) calcd. for $C_{27}H_{25}N_5$ $[M+1]^+$: 420.21, Found: 420.3, Purity: 96.3%.

*5.2.2.14. 4-((2-phenyl-6-((pyridin-2-ylmethyl)amino)pyrimidin-4-yl)amino)benzonitrile (**21**).* The title compound was synthesized from 4-((6-chloro-2-phenylpyrimidin-4-yl)amino)benzonitrile (95 mg, 0.31 mmol) and 2-picolylamine (585 mg, 5.39 mmol) as described in the general procedure of method A. Grey solid (22.0 mg, 18.8%). ^{1}H NMR (500 MHz, DMSO-d_6) δ: 9.60 (s, 1H), 8.54 (d, J = 4.3 Hz, 1H), 8.26 (dd, J = 3.0, 6.6 Hz, 2H), 7.90−7.87 (m, 2H), 7.80−7.71 (m, 4H), 7.48−7.44 (m, 3H), 7.39 (d, J = 7.9 Hz, 1H), 7.26 (dd, J = 5.0, 7.3 Hz, 1H), 5.91 (s, 1H), 4.68 (s, 2H). ^{13}C NMR (126 MHz, DMSO) δ: 163.17, 162.23, 159.81, 159.25, 148.85, 145.54, 138.15, 136.67, 133.05, 130.10, 128.21, 127.54, 122.00, 121.01, 119.56, 118.33, 101.69, 45.93. LC-MS (m/z) calcd. for $C_{23}H_{18}N_6$ $[M+1]^+$: 379.16, Found: 379.3, Purity: 98.5%.

*5.2.2.15. 4-((2-phenyl-6-((pyridin-3-ylmethyl)amino)pyrimidin-4-yl)amino)benzonitrile (**22**).* The title compound was synthesized from 4-((6-chloro-2-phenylpyrimidin-4-yl)amino)benzonitrile (86 mg, 0.28 mmol) and 3-picolylamine (687 mg, 6.35 mmol) as described in the general procedure of method A. White solid (80.3 mg, 75.8%). ^{1}H NMR (500 MHz, DMSO-d_6) δ: 9.59 (s, 1H), 8.63 (s, 1H), 8.45 (d, J = 3.3 Hz, 1H), 8.32−8.27 (m, 2H), 7.90−7.87 (m, 2H), 7.79−7.71 (m, 4H), 7.50−7.46 (m, 3H), 7.36 (ddd, J = 0.9, 4.7, 7.9 Hz, 1H), 5.89 (s, 1H), 4.63 (s, 2H). ^{13}C NMR (126 MHz, DMSO) δ: 163.00, 162.28, 159.75, 148.82, 148.00, 145.51, 138.15, 134.99, 133.07, 130.15, 128.25, 127.56, 123.46, 119.56, 118.36, 101.73, 85.15, 41.45. LC-MS (m/z) calcd. for $C_{23}H_{18}N_6$ $[M+1]^+$: 379.16, Found: 379.3, Purity: 98.9%.

*5.2.2.16. 4-((2-phenyl-6-((pyridin-4-ylmethyl)amino)pyrimidin-4-yl)amino)benzonitrile (**23**).* The title compound was synthesized from 4-((6-chloro-2-phenylpyrimidin-4-yl)amino)benzonitrile (86 mg, 0.28 mmol) and 4-picolylamine (861 mg, 7.96 mmol) as described in the general procedure of method A. White solid (74.2 mg, 69.5%). ^{1}H NMR (500 MHz, DMSO-d_6) δ: 9.60 (s, 1H), 8.52−8.50 (m, 2H), 8.25 (dd, J = 3.0, 6.3 Hz, 2H), 7.90−7.87 (m, 2H), 7.80 (t, J = 6.1 Hz, 1H), 7.75−7.71 (m, 2H), 7.48−7.44 (m, 3H), 7.38−7.35 (m, 2H), 5.89 (s, 1H), 4.63 (s, 2H). ^{13}C NMR (126 MHz, DMSO) δ: 163.09, 162.28, 149.51, 145.48, 138.09, 133.07, 130.15, 128.23, 127.54, 122.09, 119.55, 118.37, 101.76, 42.98. LC-MS (m/z) calcd. for $C_{23}H_{18}N_6$ $[M+1]^+$: 379.16, Found: 379.3, Purity: 98.5%.

*5.2.2.17. 4-((6-((2-hydroxyphenyl)amino)-2-phenylpyrimidin-4-yl) amino)benzonitrile (**24**).* The title compound was synthesized from 4-((6-chloro-2-phenylpyrimidin-4-yl)amino)benzonitrile (102 mg, 0.33 mmol) and 2-hydroxyaniline (222 mg, 2.03 mmol) as described in the general procedure of method C. Yellow solid (48.8 mg, 38.6%). ^{1}H NMR (500 MHz, DMSO-d_6) δ: 9.60 (s, 1H), 8.36 (dd, J = 3.0, 6.6 Hz, 2H), 7.91−7.87 (m, 2H), 7.78−7.71 (m, 3H), 7.52−7.47 (m, 3H), 7.36 (dd, J = 1.3, 5.0 Hz, 1H), 7.07 (dd, J = 1.3, 3.5 Hz, 1H), 6.97 (dd, J = 3.4, 5.1 Hz, 1H), 5.90 (s, 1H), 4.78 (s, 2H). ^{13}C NMR (126 MHz, DMSO) δ: 162.77, 162.20, 159.71, 145.54, 143.35, 138.16, 133.36, 133.06, 130.15, 128.24, 127.64, 126.54, 125.19, 124.88, 119.57, 118.35, 113.41, 101.70, 85.28. LC-MS (m/z) calcd. for $C_{23}H_{17}N_5O$ $[M+1]^+$: 380.14, Found: 380.1, Purity: 95.9%.

*5.2.2.18. 4-((6-((3-hydroxyphenyl)amino)-2-phenylpyrimidin-4-yl) amino)benzonitrile (**25**).* The title compound was synthesized from 4-((6-chloro-2-phenylpyrimidin-4-yl)amino)benzonitrile (106 mg, 0.34 mmol) and 3-hydroxyaniline (290 mg, 2.65 mmol) as described in the general procedure of method C. Grey solid (67.1 mg, 51.4%). ^{1}H NMR (500 MHz, DMSO-d_6) δ: 9.76 (s, 1H), 9.38 (s, 1H), 9.24 (s, 1H), 8.37−8.33 (m, 2H), 7.94−7.91 (m, 2H), 7.78−7.75 (m, 2H), 7.56−7.50 (m, 3H), 7.16−7.12 (m, 2H), 7.06 (ddd, J = 1.0, 2.0, 8.1 Hz, 1H), 6.46 (ddd, J = 1.0, 2.4, 8.0 Hz, 1H), 6.23 (s, 1H). ^{13}C NMR (126 MHz, DMSO) δ: 162.63, 161.13, 160.13, 157.75, 145.29, 141.25, 138.04, 133.13, 130.35, 129.41, 128.39, 127.70, 119.51, 118.57, 110.97, 109.45, 107.26, 102.07, 86.91. LC-MS (m/z) calcd. for $C_{23}H_{17}N_5O$ $[M+1]^+$: 380.14, Found: 380.1, Purity: 99.0%.

*5.2.2.19. 4-((6-((4-hydroxyphenyl)amino)-2-phenylpyrimidin-4-yl) amino)benzonitrile (**26**).* The title compound was synthesized from 4-((6-chloro-2-phenylpyrimidin-4-yl)amino)benzonitrile (101 mg, 0.33 mmol) and 4-hydroxyaniline (390 mg, 3.57 mmol) as described in the general procedure of method C. Grey solid (22.7 mg, 18.2%). ^{1}H NMR (500 MHz, DMSO-d_6) δ: 9.66 (s, 1H), 9.22 (s, 1H), 8.98 (s, 1H), 8.34−8.30 (m, 2H), 7.93−7.90 (m, 2H), 7.76−7.73 (m, 2H), 7.54−7.48 (m, 3H), 7.33 (d, J = 8.3 Hz, 2H), 6.81−6.78 (m, 2H), 6.02 (s, 1H). ^{13}C NMR (126 MHz, DMSO) δ: 162.54, 161.87, 160.13, 153.51, 145.41, 138.14, 133.09, 131.11, 130.22, 128.33, 127.58, 123.52, 119.54, 118.41, 115.41, 101.86, 85.41. LC-MS (m/z) calcd. for $C_{23}H_{17}N_5O$ $[M+1]^+$: 380.14, Found: 380.1, Purity: 96.5%.

*5.2.2.20. 4,4'-((2-phenylpyrimidine-4,6-diyl)bis(azanediyl))dibenzonitrile (**27**).* The title compound was the side product in synthesis of 4-((6-chloro-2-phenylpyrimidin-4-yl)amino)benzonitrile. Yellow solid. ^{1}H NMR (500 MHz, DMSO-d_6) δ: 9.92 (s, 2H), 8.34 (dd, J = 3.0, 6.7 Hz, 2H), 7.96−7.92 (m, 4H), 7.81−7.77 (m, 4H), 7.55 (dd, J = 2.0, 5.0 Hz, 3H), 6.32 (s, 1H). ^{13}C NMR (126 MHz, DMSO) δ: 162.71, 160.33, 144.92, 137.71, 133.18, 130.64, 128.57, 127.72, 119.42, 118.88, 102.57, 88.87. LC-MS (m/z) calcd. for $C_{24}H_{16}N_6$ $[M+1]^+$: 389.14, Found: 389.2, Purity: 98.2%.

5.3. Biological investigation

5.3.1. Cell culture

The MDCK II BCRP cell line transfected with ABCG2 and the corresponding wild type cell line (MDCK II) were a generous gift by Dr. A. Schinkel (The Netherlands Cancer Institute, Amsterdam, The Netherlands). Cultivation was carried out in Dulbecco's modified Eagle's medium (DMEM; Sigma Life Science, Steinheim, Germany) supplemented with FCS (10%; PAN-Biotech GmbH, Aidenbach, Germany), L-glutamine (2 mM; PAN-Biotech GmbH, Aidenbach, Germany), penicillin G (50 U/ml; PAN-Biotech GmbH, Aidenbach, Germany), and streptomycin (50 μg/mL; PAN-Biotech GmbH, Aidenbach, Germany). The human ovarian carcinoma cell line A2780/ADR (ECACC no. 931125120) overexpressing ABCB1 and the non-selected wild type cell line A2780 (ECACC no. 93112519) were purchased from European Collection of Animal Cell Culture (ECACC). RPMI-1640 medium with additional FCS (10%; PAN-

Biotech GmbH, Aidenbach, Germany), L-glutamine (2 mM), penicillin G (50 U/ml), and streptomycin (50 μg/mL) was used for cultivation. The small-cell lung cancer cell line H69AR (ATCC CRL-11351) and the corresponding parental H69 cell line (NCL-H69, ATCC HTB-119) were provided by American Type Culture Collection (ATCC). Cultivation was performed using RPMI-1640 medium supplemented with FCS (20%; PAN-Biotech GmbH, Aidenbach, Germany), L-glutamine (2 mM), penicillin G (50 U/ml), and streptomycin (50 μg/mL). For subculturing or biological assays, over 90% confluence was required in T75 cell culture flasks (Greiner Bio-One, Frickenhausen, Germany) stored under a 5% CO_2-humidified atmosphere at 37 °C in an incubator (Münchener Medizin Mechanik GmbH, Planegg, Germany). The cell layer was rinsed three times with phosphate-buffered saline (PAN-Biotech GmbH, Aidenbach, Germany) and subsequently exposed to trypsin/EDTA solution (0.05%/0.02%; PAN-Biotech GmbH, Aidenbach, Germany). Detached cells were collected in a 50 mL falcon tube and centrifuged (266×*g*; 4 °C; 4 min). The supernatant was replaced by fresh medium and the cell count was determined by CASY TT (Schärfe System GmbH, Reutlingen, Germany) equipped with a 150 μm capillary. Long-term storage of cells was conducted in a medium/DMSO mixture (90%/10%) under liquid nitrogen.

5.3.2. Pheophorbide A accumulation assay to investigate ABCG2 inhibition

Pheophorbide A assay was applied in order to determine the inhibitory potency of the compounds toward ABCG2 as described earlier with minor deviations [15–17,40,41]. First, the dilution series of the tested compound was prepared using concentrations in the range of 0.316–100 μM. These solutions were then pipetted into a flat-bottom 96 well plate (Thermo Scientific, Waltham, MA, USA). After harvesting the MDCK II BCRP cells as described earlier, 160 μL of cell suspension in KHB buffer containing approximately 45,000 cells were added to each well. Following the addition of 20 μL of 5 μM pheophorbide A solution, the plate was kept in the incubator for 2 h at 37 °C and 5% CO_2. Afterward, flow cytometry (Guava easyCyte™ HT) was applied to measure fluorescence at excitation wavelength of 488 nm and detection wavelength of 695/50 nm. Compound **28** was used as reference and for the level of possible total inhibition. Four-parameter logistic equation with variable hill slope or three-parameter logistic equation with fixed slope (=1), whatever was statistically preferred, was used to generate concentration-response curves and IC_{50} values were calculated with GraphPad Prism (version 6.0 for Windows; San Diego, CA, USA).

5.3.3. Calcein AM accumulation assay to investigate ABCB1 and ABCC1 inhibition

Calcein AM assay was applied to investigate inhibitory activity of the compounds toward ABCB1 and ABCC1 using A2780/ADR and H69AR cell lines, respectively. The accumulation assay was performed as described before with minor deviations [15–17,40,41]. Different dilutions of the test compounds (20 μL) either at 100 μM for the screening or between 0.316 μM and 100 μM for the determination of the IC_{50} value were pipetted into a clear F bottom 96-well microplate (Greiner bio one, Frickenhausen, Germany). Cell suspension was obtained as described above and 160 μL were added to the plate with either 30,000 (ABCB1) or 60,000 (ABCC1) cells per well. After an incubation period of 30 min under CO_2-humidified atmosphere (5%/37 °C), 20 μL of 3.125 μM calcein AM solution were added to the wells and the plate was immediately measured in a Fluostar Optima or Polarstar microplate reader (BMG-Labtech, Software versions 2.00R2/2.20 and 4.11-0, respectively). The fluorescence was recorded every 60 s for a time period of 1 h at the excitation wavelength of 485 nm and emission wavelength of 520 nm. The initial linear increase in fluorescence was calculated as a slope between minutes 5 and 30 and compared to the slope of cyclosporine A at a concentration of 10 μM. Only candidates that reached more than 20% inhibition level were further evaluated with complete concentration-response curves. If the curve lacked the top values, the maximal effect of cyclospine A (10 μM) was used to constrain the concentration-response curve. Four-parameter logistic equation with variable hill slope or three-parameter logistic equation with fixed slope (=1), whatever was statistically preferred, was used to generate concentration-response curves and IC_{50} values were calculated with GraphPad Prism (version 6.0 for Windows; San Diego, CA, USA).

5.3.4. Cytotoxicity assay

Intrinsic cytotoxicity of the compounds was examined with an MTT-based assay as described before with minor deviations [15–17,40,41]. A dilution series of the compounds in the range of 3.16 μM to 1 mM was prepared using culture medium as a solvent. Cells were harvested as described before and a cell suspension was prepared using MDCK II (2000 cells per well), MDCK II BCRP (2000 cells per well), A2780 (8000 cells per well), A2780/ADR (8000 cells per well), or H69AR (20,000 cells per well). To the 20 μL of the compound dilution, 180 μL of cell suspension were added to a 96-well tissue-culture treated plate (Starlab GmbH, Hamburg, Germany) and incubated for 72 h at 37 °C and 5% CO_2. Culture medium and DMSO defined 100% and 0% of cell viability, respectively. At the end of the incubation period, 40 μL of a 5 mg/mL MTT solution were added to each well and incubated for another 60 min (37 °C, 5% CO_2). After removing the supernatant, the formazan crystals were solved in 100 μL of DMSO and the absorbance was measured applying a Multiscan microplate photometer (Thermo Fischer Scientific, Waltham, MA, USA) at 570 nm with a background correction at 690 nm. Concentration-effect curves were obtained by plotting the absorbance values against logarithmic concentrations of the test compounds in GraphPad Prism and generating a curve on the basis of the four-parameter logistic equation with variable hill slope.

5.3.5. MDR reversal assay

The ability of the test compounds to reverse MDR was investigated with a different version of a MTT assay as described before with minor deviations [15–17,40,41]. Test compounds were diluted with culture medium to necessary concentrations (depending on the inhibitory activity in the respective cell line) and pipetted into a 96-well tissue-culture plate (Starlab GmbH, Hamburg, Germany). Cells were harvested as described before and 160 μL of cell suspension were added to the plate at a concentration of 2000 (MDCK II), 8000 (A2780), or 20,000 (H69) cells per well. Additionally, 20 μL of a dilution series (100 nM–100 μM) of a cytotoxic drug (SN-38 for ABCG2, daunorubicin for ABCB1 and ABCC1) were pipetted into the solution and incubated for 72 h (37 °C, 5% CO_2). Culture medium and DMSO (10%) defined 100% and 0% cell viability, respectively. After the incubation period, the procedure was the same as described for the cytotoxicity MTT assay.

Declaration of competing interest

The authors declare that they have no known competing financial interests or personal relationships that could have appeared to influence the work reported in this paper.

Acknowledgements

JL was supported by the China Scholarship Council (CSC). VN thanks BioSolveIT GmbH (Germany) for providing the evaluation

license of LeadIT. SMS receives a Walter Benjamin fellowship of the Deutsche Forschungsgemeinschaft (DFG, German Research Foundation; STE2931/2).

Appendix A. Supplementary data

Supplementary data to this article can be found online at https://doi.org/10.1016/j.ejmech.2020.113045.

References

[1] L. Amiri-Kordestani, A. Basseville, K. Kurdziel, A.T. Jojo, S.E. Bates, Targeting MDR in breast and lung cancer: discriminating its potential importance from the failure of drug resistance reversal studies, Drug Resist. Updates 15 (2012) 50–61, https://doi.org/10.1016/j.drup.2012.02.002.

[2] S.H. Lee, H. Kim, J.-H. Hwang, H.S. Lee, J.Y. Cho, Y.-S. Yoon, H.-S. Han, Breast cancer resistance protein expression is associated with early recurrence and decreased survival in resectable pancreatic cancer patients, Pathol. Int. 62 (2012) 167–175, https://doi.org/10.1111/j.1440-1827.2011.02772.x.

[3] D. Damiani, M. Tribelli, E. Calistri, A. Geromin, A. Chiarvesio, A. Michelutti, M. Cavallin R. Fanin, The prognostic value of P-glycoprotein (ABCB) and breast cancer resistance protein (ABCG2) in adults with de novo acute myeloid leukemia with normal karyotype, Haematologica 91 (2006) 825–828, https://doi.org/10.3324/%25x.

[4] D. Steinbach, W. Sell, A. Voigt, J. Hermann, F. Zintl, A. Sauerbrey, BCRP gene expression is associated with a poor response to remission induction therapy in childhood acute myeloid leukemia, Leukemia 16 (2002) 1443–1447, https://doi.org/10.1038/sj.leu.2402541.

[5] K. Matsuo, M.L. Eno, E.H. Ahn, M.M. Shahzad, D.D. Im, N.B. Rosenein, A.K. Sood, Multidrug resistance gene (MDR-1) and risk of brain metastasis in epithelial ovarian, fallopian tube, and peritoneal cancer, Am. J. Clin. Oncol. 34 (2011) 488–493, https://doi.org/10.1097/COC.0b013e3181ec5f4b.

[6] R.W. Robey, O. Polgar, J. Deeken, K.W. To, S.E. Bates, ABCG2: determining its relevance in clinical drug resistance, Canc. Metastasis Rev. 26 (2007) 39–57, https://doi.org/10.1007/s10555-007-9042-6.

[7] G. Szakacs, J.K. Paterson, J.A. Ludwig, C. Booth-Genthe, M.M. Gottesmann, Targeting multidrug resistance in cancer, Nat. Rev. Drug Discov. 5 (2006) 219–234, https://doi.org/10.1038/nrd1984.

[8] Q. Mao, J.D. Unadkat, Role of the breast cancer resistance protein (BCRP/ABCG2) in drug transport – an update, AAPS J. 17 (2015) 65–82, https://doi.org/10.1208/s12248-014-9668-6.

[9] C. Erlichman, S.A. Boerner, C.G. Hallgren, R. Spieker, X.-Y. Wang, C.D. James, G.L. Scheffer, M. Maliepaard, D.D. Ross, K.C. Bible, S.H. Kaufmann, The HER tyrosine kinase inhibitor CI1033 enhances cytotoxicity of 6-ethyl-10-hydroxycamptrothecin and topotecan by inhibiting breast cancer resistance-mediated drug efflux, Canc. Res. 61 (2001) 739–748.

[10] K.K.W. To, D.C. Poon, Y. Wei, F. Wang, G. Lin, L. Fu, Pelitinib (EKB-569) targets the up-regulation of ABCB1 and ABCG2 induced by hyperthermia to eradicate lung cancer, Br. J. Pharmacol. 172 (2015) 4089–4106, https://doi.org/10.1111/bph.13189.

[11] J. Hu, X. Zhang, F. Wang, X. Wang, K. Yang, M. Xu, K.K.W. To, Q. Li, L. Fu, Effect of ceritinib (LDK378) on enhancement of chemotherapeutic agents in ABCB1 and ABCG2 overexpressing cells in vitro and in vivo, Oncotarget 6 (2015) 44643–44659, https://doi.org/10.18632/oncotarget.5989.

[12] Y.-J. Mi, Y.-J. Liang, H.-B. Huang, H.-Y. Zhao, C.-P. Wu, F. Wang, L.-Y. Tao, C.-Z. Zhang, C.-L. Dai, A.K. Tiwari, X.-X. Ma, K.K.W. To, S.V. Ambudkar, Z.-S. Chen, L.-W. Fu, Apatinib (YN968D1) reverses multidrug resistance by inhibiting the efflux function of multiple ATP-binding cassette transporters, Canc. Res. 70 (2010) 7980–7991, https://doi.org/10.1158/0008-5472.CAN-10-0111.

[13] C.-L. Dai, Y.-J. Liang, Y.-S. Wang, A.K. Tiwari, Y.-Y. Yan, F. Wang, Z.-S. Chen, X.-Z. Tong, L.-W. Fu, Sensitization of ABCG2-overexpressing cells to conventional chemotherapeutic agent by sunitinib was associated with inhibiting the function of ABCG2, Canc. Lett. 279 (2009) 74–83, https://doi.org/10.1016/j.canlet.2009.01.027.

[14] K.K.W. To, D.C. Poon, Y. Wei, F. Wang, G. Lin, L.-W. Fu, Vatalanib sensitizes ABCB1 and ABCG2-overexpressing multidrug resistant colon cancer cells to chemotherapy under hypoxia, Biochem. Pharmacol. 97 (2015) 27–37, https://doi.org/10.1016/j.bcp.2015.06.034.

[15] K. Stefan, S.M. Schmitt, M. Wiese, 9-Deazapurines as broad-spectrum inhibitors of the ABC transport proteins P-glycoprotein, multidrug resistance-associated protein 1, and breast cancer resistance protein, J. Med. Chem. 60 (2017) 8758–8780, https://doi.org/10.1021/acs.jmedchem.7b00788.

[16] K. Silbermann, S.M. Stefan, R. Elshawadfy, V. Namasivayam, M. Wiese, Identification of thienopyrimidine scaffold as inhibitor of the ABC transport protein ABCC1 (MRP1) and related transporters using a combined virtual screening approach, J. Med. Chem. 62 (2019) 4383–4400, https://doi.org/10.1021/acs.jmedchem.8b01821.

[17] K. Silbermann, J. Li, V. Namasivayam, F. Baltes, G. Bendas, S.M. Stefan, M. Wiese, Superior pyrimidine derivatives as selective ABCG2 inhibitors and broad-spectrum ABCB1, ABCC1, and ABCG2 antagonists, J. Med. Chem. 63 (2020) 10412–10432, https://doi.org/10.1021/acs.jmedchem.0c00961.

[18] J. Yuan, I.L. Wong, T. Jiang, S.W. Wang, T. Liu, B.J. Wen, L.M. Chow, B. Wan Sheng, Synthesis of methylated quercetin derivatives and their reversal activities on P-gp- and BCRP-mediated multidrug resistance tumour cells, Eur. J. Med. Chem. 54 (2012) 413–422, https://doi.org/10.1016/j.ejmech.2012.05.026.

[19] L. Cheung, C.L. Flemming, F. Watt, N. Masada, D.M.T. Yu, T. Huynh, G. Conseil, A. Tivnan, A. Polinsky, A.V. Gudkov, M.A. Munoz, A. Vishvanath, D.M.F. Cooper, M.J. Henderson, S.P.C. Cole, J.I. Fletcher, M. Haber, M.D. Norris, High-throughput screening identifies ceefourin 1 and ceefourin 2 as highly selective inhibitors of multidrug resistance protein 4 (MRP4), Biochem. Pharmacol. 91 (2014) 97–108, https://doi.org/10.1016/j.bcp.2014.05.023.

[20] Y.F. Fan, W. Zhang, L. Zeng, Z.N. Lei, C.Y. Cai, P. Gupta, D.H. Yang, Q. Cui, Z.D. Quin, Z.S. Chen, L.D. Trombetta, Dacomitinib antagonizes multidrug resistance (MDR) in cancer cells by inhibiting the efflux activity of ABCB1 and ABCG2 transporters, Canc. Lett. 421 (2018) 186–198, https://doi.org/10.1016/j.canlet.2018.01.021.

[21] W. Zhang, Y.F. Fan, C.Y. Cai, J.Q. Wang, Q.X. Teng, Z.N. Lei, L. Zeng, P. Gupta, Z.S. Chen, Olmutinib (BI1482694/HM61713), a novel epidermal growth factor receptor tyrosine kinase inhibitor, reverses ABCG2-mediated multidrug resistance in cancer cells, Front. Pharmacol. 9 (2018) 1097, https://doi.org/10.3389/fphar.2018.01097.

[22] P. Gupta, Y.K. Zhang, X.Y. Zhang, Y.J. Wang, K.W. Lu, T. Hall, R. Peng, D.H. Yang, N. Xie, Z.S. Chen, Voruciclib, a potent CDK4/6 inhibitor, antagonizes ABCB1 and ABCG2-mediated multi-drug resistance in cancer cells, Cell. Physiol. Biochem. 45 (2018) 1515–1528, https://doi.org/10.1159/000487578.

[23] X. Zhu, I.L.K. Wong, K.F. Chan, J. Cui, M.C. Law, T.C. Chong, X. Hu, L.M.C. Chow, T.H. Chan, Triazole bridged flavonoid dimers as potent, nontoxic, and highly selective breast cancer resistance protein (BCRP/ABCG2) inhibitors, J. Med. Chem. 62 (2019) 8578–8608, https://doi.org/10.1021/acs.jmedchem.9b00963.

[24] Z.X. Wu, Q.X. Teng, C.Y. Cai, J.Q. Wang, Z.N. Lei, Y. Yang, Y.F. Fan, J.Y. Zhang, J. Li, Z.S. Chen, Tepotinib reverses ABCB1-mediated multidrug resistance in cancer cells, Biochem. Pharmacol. 166 (2019) 120–127, https://doi.org/10.1016/j.bcp.2019.05.015.

[25] L. Wang, L. Liang, T. Yang, Y. Qiao, Y. Xia, L. Liu, C. Li, P. Lu, X. Jiang, A pilot clinical study of apatinib plus irinotecan in patients with recurrents high-grade glioma, Medicine (Baltim.) 96 (2017) 1–5, https://doi.org/10.1097/MD.0000000000009053, e9053.

[26] M.K. Krapf, J. Gallus, V. Namasivayam, M. Wiese, 2,4,6-Substituted quinazolines with extraordinary inhibitory potency toward ABCG2, J. Med. Chem. 61 (2018) 7952–7976, https://doi.org/10.1021/acs.jmedchem.8b01011.

[27] M.K. Krapf, M. Wiese, Synthesis and biological evaluation of 4-anilino-quinazolines and –quinolines as inhibitors of breast cancer resistance protein (ABCG2), J. Med. Chem. 59 (2016) 5449–5461, https://doi.org/10.1021/acs.jmedchem.6b00330.

[28] C. Ozvegy-Laczka, T. Hegedus, G. Varady, O. Ujhelly, J.D. Schuetz, A. Varadi, G. Keri, L. Orfi, K. Nemet, B. Sarkadi, High-affinity interaction of tyrosine kinase inhibitors with the ABCG2 multidrug transporter, Mol. Pharmacol. 65 (2004) 1485–1495, https://doi.org/10.1124/mol.65.6.1485.

[29] N.A. Colabufo, V. Pagliarulo, F. Berardi, M. Contino, C. Inglese, M. Niso, P. Ancona, G. Albo, A. Pagliarulo, R. Perrone, Bicalutamide failure in prostate cancer treatment: involvement of Multi Drug Resistance Proteins, Eur. J. Pharmacol. 601 (2008) 38–42, https://doi.org/10.1016/j.ejphar.2008.10.038.

[30] N.A. Colabufo, F. Berardi, M.G. Perrone, M. Cantore, M. Contino, C. Inglese, M. Niso, R. Perrone, Multi-drug-resistance-reverting agents: 2-aryloxazole and 2-arylthiazole derivatives as potent BCRP and MRP1 inhibitors, ChemMedChem 4 (2009) 188–195, https://doi.org/10.1002/cmdc.200800329.

[31] C.L. Dai, A.K. Tiwari, C.P. Wu, X.D. Su, S.R. Wang, D.G. Liu, C.R. Ashby Jr., Y. Huang, R.W. Robey, Y.J. Liang, L.M. Chen, C.J. Shi, S.V. Ambudkar, Z.S. Chen, L.W. Fu, Lapatinib (Tykerb, GW572016) reverses multidrug resistance in cancer cells by inhibiting the activity of ATP-binding cassette subfamily B member 1 and G member 2, Canc. Res. 68 (2008) 7905–7914, https://doi.org/10.1158/0008-5472.CAN-08-0499.

[32] S.L. Ma, Y.P. Hu, F. Wang, Z.C. Huang, Y.F. Chen, X.K. Wang, L.W. Fu, Lapatinib antagonizes multidrug resistance-associated protein 1-mediated multidrug resistance by inhibiting its transport function, Mol. Med. 20 (2014) 390–399, https://doi.org/10.2119/molmed.2014.00059.

[33] K. Juvale, K. Stefan, M. Wiese, Synthesis and biological evaluation of flavones and benzoflavones as inhibitors of BCRP/ABCG2, Eur. J. Med. Chem. 67 (2013) 115–126, https://doi.org/10.1016/j.ejmech.2013.06.035.

[34] A. Krauze, S. Grinberga, L. Krasnova, I. Adlere, E. Sokolova, I. Domracheva, I. Shestakova, Z. Andzans, G. Duburs, Thieno[3,2-b]pyridines–a new class of multidrug resistance (MDR) modulators, Bioorg. Med. Chem. 22 (2014) 5860–5870, https://doi.org/10.1016/j.bmc.2014.09.023.

[35] E. Teodori, M. Contino, C. Riganti, G. Bartolucci, L. Braconi, D. Manetti, M.N. Manetti, A. Trezza, A. Athanasios, O. Spiga, M.G. Perrone, R. Giampietro, E. Gazzano, M. Salerno, N.A. Colabufo, S. Dei, Design, synthesis and biological evaluation of stereo- and regioisomers of amino aryl esters as multidrug resistance (MDR) reversers, Eur. J. Med. Chem. 182 (2019) 111655, https://doi.org/10.1016/j.ejmech.2019.111655.

[36] F. Antoni, D. Wifling, G. Bernhardt, Water-soluble inhibitors of ABCG2 – a fragment-based and computational approach, Eur. J. Med. Chem. (2020), https://doi.org/10.1016/j.emech.2020.112958. In press.

[37] M.K. Krapf, J. Gallus, M. Wiese, 4-Anilino-2-pyridylquinazolines and –pyrimidines as highly potent and nontoxic inhibitors of breast cancer resistance protein (ABCG2), J. Med. Chem. 60 (2017) 4474–4495, https://

doi.org/10.1021/acs.jmedchem.7b00441.
[38] N.M.I. Taylor, I. Manolaridis, S.M. Jackson, J. Kowal, H. Stahlberg, K.P. Locher, Structure of the human multidrug transporter ABCG2, Nature 546 (2017) 504–509, https://doi.org/10.1038/nature22345.
[39] S.M. Jackson, I. Manolaridis, J. Kowal, M. Zechner, N.M.I. Taylor, M. Bause, S. Bause, R. Bartholomaeus, G. Bernhardt, B. Koenig, A. Buschauer, H. Stahlberg, K.H. Altmann, K.P. Locher, Structural basis of small-molecule inhibition of human multidrug transporter ABCG2, Nat. Struct. Mol. Biol. 25 (2018) 333–340, https://doi.org/10.1038/s41594-018-0049-1.
[40] S.M. Schmitt, K. Stefan, M. Wiese, Pyrrolopyrimidine derivatives as novel inhibitors of multidrug resistance-associated protein 1, J. Med. Chem. 59 (2016) 3018–3033, https://doi.org/10.1021/acs.jmedchem.5b01644.
[41] K. Silbermann, C.P. Shah, N.U. Sahu, K. Juvale, S.M. Stefan, P.S. Kharkar, M. Wiese, Novel chalcone and flavone derivatives as selective and dual inhibitors of the transport proteins ABCB1 and ABCG2, Eur. J. Med. Chem. 164 (2019) 193–213, https://doi.org/10.1016/j.ejmech.2018.12.019.
[42] M.K. Krapf, J. Gallus, M. Wiese, Synthesis and biological investigation of 2,4-substituted quinazolines as highly potent inhibitors of breast cancer resistance protein (ABCG2), Eur. J. Med. Chem. 139 (2017) 587–611, https://doi.org/10.1016/j.ejmech.2017.08.020.
[43] S.M. Stefan, Multi-target ABC transporter modulators: what next and where to go? Future Med. Chem. 11 (2019) 2353–2358, https://doi.org/10.4155/fmc-2019-0185.
[44] A. Ahmed-Belkacem, A. Pozza, S. Macalou, J.M. Perez-Victoria, A. Boumendjel, A. Di Pietro, Inhibitors of cancer cell multidrug resistance mediated by breast cancer resistance protein (BCRP/ABCG2), Anti Canc. Drugs 17 (2006) 239–243, https://doi.org/10.1097/00001813-200603000-00001.
[45] M. Contino, S. Guglielmo, M.G. Perrone, R. Giampietro, B. Rolando, A> Carrieri, D. Zaccaria, K. Chegaev, V. Borio, C. Riganti, K. Zabielska-Koczywas, N.A. Colabufo, R. Fruttero, New tetrahydroisoquinoline-based P-glycoprotein modulators: decoration of the biphenyl core gives selective ligands, Med. Chem. Comm. 9 (2018) 862–869, https://doi.org/10.1039/c8md00075a.
[46] S. Ranjbar, R. Khonkarn, A. Moreno, H. Baubichon-Sortay, R. Miri, M. Khoshneviszadeh, L. Saso, N. Edraki, P. Falson, O. Firuzi, 5-Oxo-hexahydroquinioline derivatives as modulators of P-gp, MRP1 and BCRP transporters to overcome multidrug resistance in cancer cells, Toxicol. Appl. Pharmacol. 362 (2019) 136–149, https://doi.org/10.1016/j.taap.2018.10.025.
[47] K. Stefan, L.Y.W. Leck, V. Namasivayam, P. Bascuñana, M.L.-H. Huang, P.J. Riss, J. Pahnke, P.J. Jansson, S.M. Stefan, Vesicular ATP-binding cassette transporters in human disease: relevant aspects of their organization for future drug development, Future Drug Discov. 2 (2020) FDD51, https://doi.org/10.4155/fdd-2020-0025.
[48] A. Pawarode, S. Shukla, H. Minderman, S.M. Fricke, E.M. Pinder, K.L. O'Loughlin, S.V. Ambudkar, M.R. Baer, Differential effects of the immunosuppressive agents cyclosporine A, tacrolimus and sirolimus on drug transport by multidrug resistance proteins, Canc. Chemother. Pharmacol. 60 (2007) 179–188, https://doi.org/10.1007/s00280-006-0357-8.
[49] I. Ivnitski-Steele, R.S. Larson, D.M. Lovato, H.M. Khawaja, S.S. Winter, T.I. Oprea, L.A. Sklar, B.S. Edwards, High-throughput flow cytometry to detect selective inhibitors of ABCB1, ABCC1, and ABCG2 transporters, Assay Drug Dev. Technol. 6 (2008) 263–276, https://doi.org/10.1089/adt.2007.107.
[50] A. Pick, W. Klinkhammer, M. Wiese, Specific inhibitors of the breast cancer resistance protein (BCRP), ChemMedChem 5 (2010) 1498–1505, https://doi.org/10.1002/cmdc.201000216.
[51] Y.-J. Mi, Y.-J. Liang, H.-B. Huang, H.-Y. Zhao, C.-P. Wu, F. Wang, L.-Y. Tao, C.-Z. Zhang, C.-L. Dai, A.K. Tiwari, X.-X. Ma, K.K.W. To, S.V. Ambudkar, Z.S. Chen, L.-W. Fu, Apatinib (YN968D1) reverses multidrug resistance by inhibiting the efflux function of multiple ATP-binding cassette transporters, Canc. Res. 70 (2010) 7981–7991, https://doi.org/10.1158/0008-5472.CAN-10-0111.
[52] K. Juvale, J. Gallus, M. Wiese, Investigation of quinazolines as inhibitors of breast cancer resistance proteins (ABCG2), Bioorg. Med. Chem. 21 (2013) 7858–7873, https://doi.org/10.1016/j.bmc.2013.10.007.
[53] T.J. Mathias, K. Natarjan, S. Shukla, K.A. Doshi, Z.N. Singh, S.V. Ambudkar, M.R. Baer, The FLT3 and PDGFR inhibitor crenolanib is a substrate of the multidrug resistance protein ABCB1 but not does not inhibit transport function at pharmacologically relevant concentrations, Invest. N. Drugs 33 (2015) 300–309, https://doi.org/10.1007/s10637-015-0205.
[54] M.K. Krapf, J. Gallus, A. Spindler, M. Wiese, Synthesis and biological evaluation of quinazoline derivatives – a SAR study of novel inhibitors of ABCG2, Eur. J. Med. Chem. 161 (2019) 506–525, https://doi.org/10.1016/j.ejmech.2018.10.026.
[55] F. Antoni, M. Bause, M. Scholler, S. Bauer, S.A. Stark, S.M. Jackson, I. Manolaridis, K.P. Locher, B. König, A. Buschauer, G. Bernhardt, Tariquidar-related triazoles as potent, selective and stable inhibitors of ABCG2 (BCRP), Eur. J. Med. Chem. 191 (2020) 112133, https://doi.org/10.1016/j.ejmech.2020.112133.
[56] Molecular Operating Environment (MOE), 2018.01; Chemical Computing Group ULC: 1010 Sherbooke St. West, Suite #910, Montreal, QC, Canada, H3A 2R7, 2018.
[57] LeadIT, version 2.3.2; BioSolveIT GmbH: Sankt Augustin, Germany, 2017.
[58] M. Rarey, B. Kramer, T. Lengauer, G. Klebe, A fast flexible docking method using an incremental construction algorithm, J. Mol. Biol. 261 (1996) 470–489, https://doi.org/10.1006/jmbi.1996.0477.